

Report No. BMI-1536

UC-25 Metals, Ceramics, and  
Materials  
(TID-4500, 16th Ed.)

Contract No. W-7405-eng-92

DEVELOPMENT OF NIOBIUM-URANIUM ALLOYS  
FOR ELEVATED-TEMPERATURE  
FUEL APPLICATIONS

by

John A. DeMastry  
Donald P. Moak  
Seymour G. Epstein  
Arthur A. Bauer  
Ronald F. Dickerson

August 9, 1961

BATTELLE MEMORIAL INSTITUTE  
505 King Avenue  
Columbus 1, Ohio

## **DISCLAIMER**

**This report was prepared as an account of work sponsored by an agency of the United States Government. Neither the United States Government nor any agency Thereof, nor any of their employees, makes any warranty, express or implied, or assumes any legal liability or responsibility for the accuracy, completeness, or usefulness of any information, apparatus, product, or process disclosed, or represents that its use would not infringe privately owned rights. Reference herein to any specific commercial product, process, or service by trade name, trademark, manufacturer, or otherwise does not necessarily constitute or imply its endorsement, recommendation, or favoring by the United States Government or any agency thereof. The views and opinions of authors expressed herein do not necessarily state or reflect those of the United States Government or any agency thereof.**

## **DISCLAIMER**

**Portions of this document may be illegible in electronic image products. Images are produced from the best available original document.**

## TABLE OF CONTENTS

	<u>Page</u>
ABSTRACT . . . . .	1
INTRODUCTION . . . . .	1
ALLOY PREPARATION BY ARC CASTING . . . . .	2
FABRICATION STUDIES OF ARC-CAST ALLOYS . . . . .	4
Flat Rolling . . . . .	5
Hot Forging . . . . .	5
Rod Rolling . . . . .	6
CONSUMABLE-ELECTRODE SKULL-CASTING STUDIES . . . . .	9
Melting Studies . . . . .	12
FABRICATION STUDIES OF SKULL-CAST ALLOYS . . . . .	15
MECHANICAL-PROPERTY DETERMINATIONS . . . . .	22
Elevated-Temperature Short-Time Tensile Tests . . . . .	22
Creep Studies . . . . .	26
CORROSION-TEST RESULTS . . . . .	31
In NaK and Sodium . . . . .	31
In Water . . . . .	38
PHYSICAL-PROPERTY DETERMINATIONS . . . . .	52
Thermal-Conductivity Measurements . . . . .	52
Electrical-Resistivity Measurements . . . . .	52
Thermal-Expansion Measurements . . . . .	55
Recrystallization Studies . . . . .	55
PHASE STUDIES . . . . .	59
CONCLUSIONS . . . . .	61
ACKNOWLEDGMENTS . . . . .	62
REFERENCES . . . . .	62

## DEVELOPMENT OF NIOBIUM-URANIUM ALLOYS FOR ELEVATED-TEMPERATURE FUEL APPLICATIONS

John A. DeMastry, Donald P. Moak, Seymour G. Epstein,  
Arthur A. Bauer, and Ronald F. Dickerson

*As a continuation of studies reported in BMI-1400, fabrication characteristics, physical and mechanical properties, and corrosion behavior in NaK, sodium, and water of niobium-uranium binary alloys containing up to 60 w/o uranium were investigated.*

*Alloys were cast by a skull melting and consumable and nonconsumable arc-melting methods. Fabrication difficulties with alloys containing greater than 25 w/o uranium were related to coring-type microsegregation during casting.*

*Tensile tests indicated 0.2 per cent offset yield strengths of 16,880, 22,370, and 28,600 psi for niobium-4.38, -14.3, and -20 w/o uranium alloys, respectively, at 2000 F. Additional tensile data were obtained for alloys from 1600 to 2400 F. Stresses to produce minimum creep rates of 0.001, 0.01, and 0.1 per cent per hr at 1600, 1800, and 2000 F were also determined. Both tensile and creep strengths were found to be sensitive to oxygen content.*

*All alloys appeared compatible with NaK at 1600 F and with sodium at 1500 F. In 600 F water, most of the alloys tested exhibited negligible weight changes after 336 days' exposure. Weight changes were greater after 140 days' exposure to 680 F water, but corrosion rates were considered satisfactory for a clad fuel.*

*The thermal and electrical conductivities of niobium are lowered by the addition of uranium, while the thermal-expansion characteristics are essentially unaffected.*

*Recrystallization temperatures for 90 per cent cold-reduced niobium-4.38, -14.3, -20, -25.0, and -30 w/o uranium alloys are 2300, 2300, 2400, 2300, and 2200 F, respectively.*

*No appreciable effect of oxygen contents ranging from 100 to 1000 ppm was observed on the composition limits of the gamma immiscibility gap in the niobium-uranium system.*

### INTRODUCTION

Utilization of metallic fuel alloys at elevated temperatures is dependent upon the development of materials which have sufficient strength to resist gas pressure resulting from the accumulation of fission gases in the fuel. It is also desirable that such fuels possess sufficient strength at elevated temperature to minimize the need of structural support. The niobium-uranium system appeared to be a logical choice for development of high-temperature fuel alloys because niobium and uranium exhibit complete mutual solubility at elevated temperatures and also because niobium and niobium alloys exhibit excellent high-temperature strength. Consequently, a study was undertaken to determine whether niobium alloys containing 10 to 60 w/o uranium had the necessary qualifications of fabricability, elevated-temperature strength, compatibility with various reactor coolants, and thermal conductivity for a reactor fuel material.

The results of initial investigations of the niobium-uranium alloy system were reported in BMI-1400.(1) The conclusions indicated that niobium-uranium alloys, especially the niobium-20 w/o uranium alloy, showed excellent potential as reactor fuels. Niobium-20 w/o uranium alloy ingots were fabricated in molybdenum cans to prevent oxidation during forging at 2500 F. The alloy exhibited a 0.2 per cent offset yield strength at 1600 F of 58,100 psi with 16 per cent reduction in area. The corrosion life in 600 and 680 F water, 750 F steam, and 1600 F NaK was more than adequate for a fuel material. Alloys containing 30 w/o or more uranium were not fabricable by the techniques employed in this initial study, and the need for a more basic understanding of the fabrication characteristics of alloys was indicated.

The results of more detailed studies of niobium-uranium alloys are contained in this report. These results were obtained on alloy material prepared by three different casting techniques: nonconsumable inert-electrode arc melting, consumable-electrode arc melting, and consumable-electrode skull-casting techniques. Most of the property data were obtained on material prepared by conventional consumable-electrode arc-melting practices. Preparation and fabrication studies involving these materials are presented first in this report. Mechanical-property data were obtained on material prepared by consumable-electrode arc melting and by consumable-electrode skull-casting techniques. Since no significant effect of casting technique was noted on mechanical properties, such data from the different materials are reported in one section.

#### ALLOY PREPARATION BY ARC CASTING

The niobium used was obtained from three suppliers. Table 1 lists the analysis of the niobium which was used as the high-purity melting stock in the property studies. Niobium with two levels of zirconium contamination was also used to prepare material for property studies. Table 2 lists the analyses for niobium of high and low zirconium content. Table 3 lists analyses for niobium used to prepare alloys for rod-rolling fabrication studies, consumable-electrode skull-casting studies, and also for the investigation of the effect of oxygen on the gamma loop. The uranium used for melting stock was high-quality biscuit which contained 27 ppm oxygen and 2.1 ppm hydrogen.

Both consumable-electrode and nonconsumable inert-electrode arc melting were employed in specimen preparation.

Electrodes for consumable-electrode arc melting were prepared by welding uranium strip (rolled to a cross-section area which when attached to the niobium would give the composition desired) onto the niobium bars in a dry box (helium atmosphere). After melting, the ingots were turned on a lathe, quartered, and rewelded into an electrode which was remelted. Final ingots weighed between 3 and 4 lb each. The niobium shown in Tables 1 and 2 was used in the above operations. Ingots prepared as above containing 10 and 20 w/o uranium were then "canned" in molybdenum and forged at 2550 F to 1/2-in.-thick slabs. After forging, the slabs were decanned and rolled in air from a helium-atmosphere furnace at 1800 F to sheet material. This sheet material was vapor blasted to remove surface oxide and utilized in property determination.

(1) References at end.

TABLE 1. CHEMICAL ANALYSIS OF HIGH-PURITY  
NIOBIUM MELTING STOCK<sup>(a)</sup> USED IN  
PROPERTY STUDIES

Element	Analysis, w/o
Niobium	99.8 minimum
Oxygen	0.009 to 0.030
Nitrogen	0.020 to 0.030
Carbon	0.003 to 0.013
Titanium	0.012 to 0.015
Tantalum	0.075 to 0.082
Nickel	0.001 to 0.005
Tungsten	<0.01
Zirconium	<0.02
Iron	<0.007
Aluminum	<0.0001
Yttrium	<0.01
Lead	<0.001
Chromium	<0.001
Cobalt	<0.001
Molybdenum	<0.020
Silicon	<0.010
Boron	<0.0001
Cadmium	<0.0001
Lithium	<0.0001

(a) Obtained from Fansteel Metallurgical Corporation.

TABLE 2. CHEMICAL ANALYSIS OF HIGH- AND LOW-ZIRCONIUM  
NIOBIUM<sup>(a)</sup> USED IN PROPERTY STUDIES

Element	Analysis, w/o	
	Low Zirconium	High Zirconium
Boron	<0.001	<0.0001
Carbon	0.027	0.028
Nitrogen	0.060	0.058
Oxygen	0.070	0.060
Tantalum	0.070	0.070
Titanium	<0.005	<0.005
Iron	0.020	0.020
Silicon	0.010	0.010
Zirconium	0.17	0.74
Niobium	99.53	99.01

(a) Obtained from Kennametal, Inc.

TABLE 3. CHEMICAL ANALYSIS OF NIOBIUM MELTING STOCK<sup>(a)</sup>  
USED FOR ROD-ROLLING FABRICATION STUDIES,  
SKULL-CASTING STUDIES, AND INVESTIGATION OF  
EFFECT OF OXYGEN ON GAMMA LOOP

Element	Analysis, w/o
Aluminum	<0.0020
Boron	0.0001
Carbon	0.004
Cadmium	<0.0005
Chromium	<0.002
Copper	<0.004
Iron	0.012
Lead	<0.002
Magnesium	<0.002
Manganese	<0.002
Molybdenum	<0.002
Nitrogen	0.005
Nickel	<0.002
Niobium	>99.8
Oxygen	0.009
Silicon	<0.010
Tantalum	0.054
Tin	<0.0002
Titanium	<0.015
Vanadium	<0.002
Tungsten	0.030
Zinc	<0.002

(a) Obtained from Wah Chang Corporation.

For inert-electrode arc melting the niobium shown in Table 3 was rolled into sheet at room temperature. This sheet was then nibbled into 1/2-in. squares for melting stock. These nibbles were arc melted into buttons which were then cast into shapes for the rod-rolling and phase studies.

#### FABRICATION STUDIES OF ARC-CAST ALLOYS

The fabrication of niobium-uranium alloys was investigated by rolling flat plates, by forging, and by rod rolling. Evaluation of fabrication results reported in BMI-1400<sup>(1)</sup> suggested that higher fabrication temperatures (above 2500 F), alloying with zirconium, or possibly the use of surface lubricants such as glass could improve the fabrication characteristics of the niobium-uranium alloys. In order to evaluate fabricability at higher temperatures (2400 to 3000 F) and the effects of zirconium additions, the following studies were conducted: (1) niobium containing 30 w/o or more uranium and 0, 10, and 20 w/o zirconium additions was forged at temperatures ranging from 2400 to 3000 F; and

(2) niobium containing 10, 20, and 30 w/o uranium and niobium-30 w/o uranium-10 and -20 w/o zirconium alloys were fabricated by rod rolling. Rod-rolling and forging operations were conducted on specimens which had been canned in molybdenum packs. All fabrication was conducted between 2100 and 3000 F, inclusive. In addition to the above, the use of a lubricant was evaluated by flat rolling alloys containing 30, 40, 50, and 60 w/o uranium in a protective envelope of molten glass at 2500 F.

#### Flat Rolling

Sections of alloys containing 30, 40, 50, and 60 w/o uranium were cut from consumably arc-melted ingots and machined to rectangular slabs 1 by 3/4 by 1/2 in. In order to determine if lubricant on the surface would prevent excessive surface cracking experienced during rolling, these slabs were encased in glass. This encasement was accomplished by dipping the cold slabs into molten glass and allowing the "glass pack" to cool in air. The specimens appeared to be successfully coated as the glass adhered to the metal slabs when cooled to room temperature. The glass-coated slabs were heated to 2500 F and flat rolling was attempted.

It was found that the molten glass failed to adhere to any except the 30 w/o uranium alloy during rolling. The oxide on the surfaces of the niobium-uranium alloys, with the exception of the 30 w/o uranium alloy, was apparently incompatible with the molten glass and wetting between the glass and surface oxide did not occur. Although the 30 w/o uranium alloy was successfully coated by the glass, the fabrication was unsuccessful since surface cracking was encountered. No further attempts at fabrication utilizing glass as a lubricant were made.

#### Hot Forging

Additions of 10 and 20 w/o zirconium were made to niobium-30, -40, -50, and -60 w/o uranium alloys in an attempt to improve their fabrication characteristics. All ingots were prepared by consumable-electrode arc melting using niobium containing 300 ppm oxygen and 20 ppm zirconium. The finished ingots which weighed approximately 3 lb and were 2 in. in diameter were cut into slabs 3/4 in. thick. These slabs were then encapsulated in molybdenum cans and end plates were welded onto the cans in an inert-atmosphere dry box. These packs were then upset forged from a hydrogen-atmosphere furnace held at temperatures of 2400, 2800, and 3000 F.

The results of this fabrication study are summarized in Table 4. It appears that the addition of zirconium results in slightly increased fabricability of the 30 and 40 w/o uranium alloys. However, more improvement in fabricability appears to be gained by the reduction of fabrication temperatures from 3000 to 2400 F. A more thorough investigation of the effects of lower working temperatures on the fabricability appeared to be advisable and rod rolling was selected for this study.

TABLE 4. RESULTS OF UPSET FORGING<sup>(a)</sup> OF NIOBIUM-URANIUM AND NIOBIUM-URANIUM-ZIRCONIUM ALLOYS

Alloy Composition (Balance Niobium), w/o	Fabrication Temperature, F	Remarks
30 U	3000	Slab fractured; severe surface cracks
30 U-10 Zr	3000	Slab fractured; severe surface cracks
40 U	3000	Slab fractured
40 U-10 Zr	3000	Slab fractured
30 U	2800	Surface cracks; slab fractured into five pieces
30 U-10 Zr	2800	Surface cracks; slab fractured into three pieces
40 U-10 Zr	2800	Slab fractured into three pieces
40 U-20 Zr	2800	Slab fractured
30 U	2400	Slab fractured; slight surface cracks
30 U-10 Zr	2400	Slab in two pieces; material appears sound otherwise
40 U-10 Zr	2400	Slab in one piece; edge cracks; radiograph shows signs of slight internal cracks
40 U-20 Zr	2400	Slab fractured into two pieces; material appears to be sound otherwise

(a) Ingot was encased in evacuated molybdenum cans.

#### Rod Rolling

Rod-rolling techniques were adopted for further studies of the effects of temperature on the fabrication characteristics of the niobium-uranium and niobium-uranium-zirconium alloys. Rod rolling offers a combination of advantages not obtainable by other methods available; it permits controlled reductions, radial restraint of ingots<sup>(2)</sup>, and the use of small cast ingots. Small right circular cylinders 1/2 in. in diameter and 3 in. long were prepared by tungsten-electrode arc-melting techniques. Charges weighing 125 to 150 g were melted six times to insure homogeneity and were then cast into a right-cylinder water-cooled copper mold. These castings were prepared from niobium melting stock which contained 94 ppm oxygen. The castings were given a homogenization anneal at 2300 F for 4 hr and furnace cooled, and then they were inserted into molybdenum cans. These can assemblies, as shown in Figure 1, were reduced from a diameter of 1 in. to 3/8 in. in rod rolls.

The temperature of fabrication and the composition of the alloys which were rod rolled are shown in Table 5. Observations concerning the conditions of the alloy specimens after fabrication were made by radiographing the can assembly. Figure 2 shows radiographs of alloys rolled at 2800 F. As can be observed, the niobium-10 w/o uranium alloy is sound, the niobium-20 w/o uranium alloy shows evidence of cracking near one end, while the niobium-30 w/o uranium and niobium-30 w/o uranium-10 and -20 w/o

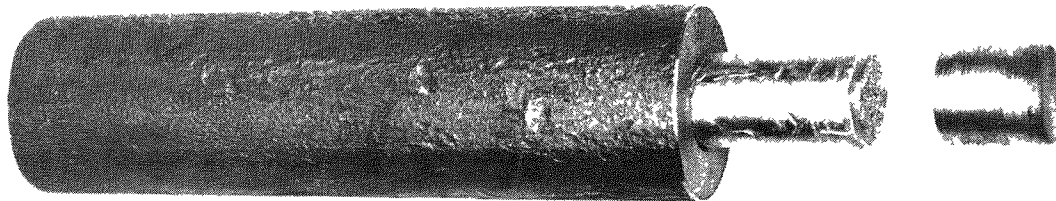


FIGURE 1. CAN ASSEMBLY

The end cap and outer tube are made of molybdenum. A portion of the casting can be seen protruding from the can. The plug shown on the extreme right is welded into place in an inert-atmosphere dry box.

TABLE 5. FABRICATION OF 1-IN.-DIAMETER CYLINDERS  
CONTAINING NIOBIUM-URANIUM AND NIOBIUM-  
URANIUM-ZIRCONIUM ALLOYS

Alloy Composition (Balance Niobium), w/o	Temperature, F	Remarks
10 U	2800	Sound rod
20 U		Ditto
30 U		Fractured
30 U-10 Zr		Ditto
30 U-20 Zr		Ditto
30 U	2400	Fractured
30 U-10 Zr		Ditto
30 U-20 Zr		Ditto
10 U	2100	Sound rod
20 U		Ditto
30 U		Fractured
30 U-10 Zr		Ditto
30 U-20 Zr		Ditto

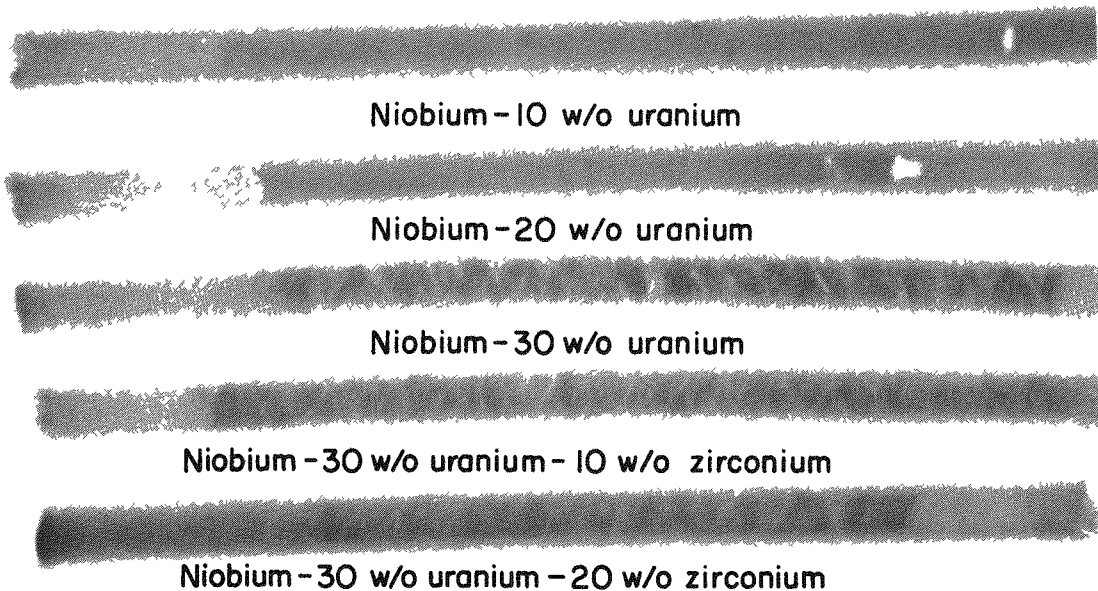


FIGURE 2. RADIOGRAPH OF NIOBIUM-URANIUM ALLOYS  
ROD ROLLED AT 2800 F

zirconium alloys are badly fractured. Examination of the fractured areas of these alloys showed areas which appeared to have been molten. Microstructural examination revealed severe coring in alloys containing 30 w/o or more uranium. On the basis of the niobium-uranium phase diagram (Figure 3)(3) and the shape of the liquidus and solidus curves, it would be expected that coring would be observed in alloys containing more than about 20 w/o uranium. Furthermore, if coring-type segregation is sufficiently severe, local areas could be molten at the higher (2800 to 3000 F) fabrication temperatures employed. At 3000 F, segregated areas containing 50 w/o uranium would be molten and areas containing 70 w/o uranium would cause localized melting at 2800 F. Since the lower-melting constituents are segregated at grain boundaries, the alloys are effectively hot short during fabrication at the higher temperatures employed in these studies. If this analysis of the fabrication problems is correct, then fabricability should be improved by lowering the temperature of working. Such improvement was indicated in material which was upset forged, as seen previously in Table 4.

In an effort to further determine if the above analysis was correct, several alloys were fabricated at both 2400 and 2100 F. Although the results of rolling the niobium-30 w/o uranium alloy at 2400 F were generally better than those obtained by working at 2800 F, the results were still unacceptable. Figure 4 shows a radiograph of the can assembly containing the niobium-30 w/o uranium alloy after fabrication at 2400 F. While the cracks appear larger, the number of cracks is less than obtained at 2800 F. At 2100 F, material was produced which contained still fewer cracks than did material fabricated at the higher temperatures. Despite the improvement, however, fabricability was still poor.

It appears that segregation is the main deterrent to successful fabrication of niobium-uranium alloys containing more than 30 w/o uranium. The high strength of these alloys makes high temperatures a requisite for fabrication while coring limits the fabrication temperatures which may be employed without rendering the alloy hot short. Obviously, it would be desirable to produce a more homogeneous alloy for fabrication. However, diffusion rates in the niobium-uranium system are quite low until temperatures close to the melting point are achieved. As reported in a later section on phase studies, attempts to homogenize niobium-uranium alloys by annealing at temperatures ranging from 1200 to 1600 C for 8 hr were unsuccessful. Consequently, attempts to improve alloy homogeneity were restricted to attempts to improve the cast product by means of consumable-electrode skull casting.

#### CONSUMABLE-ELECTRODE SKULL-CASTING STUDIES

With conventional consumable-electrode arc melting segregation has been observed both in the form of microsegregation, resulting from the wide liquidus-solidus temperature range (Figure 3) for the high-uranium alloys, and as macrosegregation in the form of banding. This banding appears to result from the density differences between niobium and uranium as well as wander and fluctuation of the arc during conventional arc melting.(4)

In an attempt to produce niobium alloys containing 30 w/o or more uranium with structures amenable to fabrication, skull-melting techniques were investigated. Six ingots with compositions varying from pure niobium to niobium-50 w/o uranium were

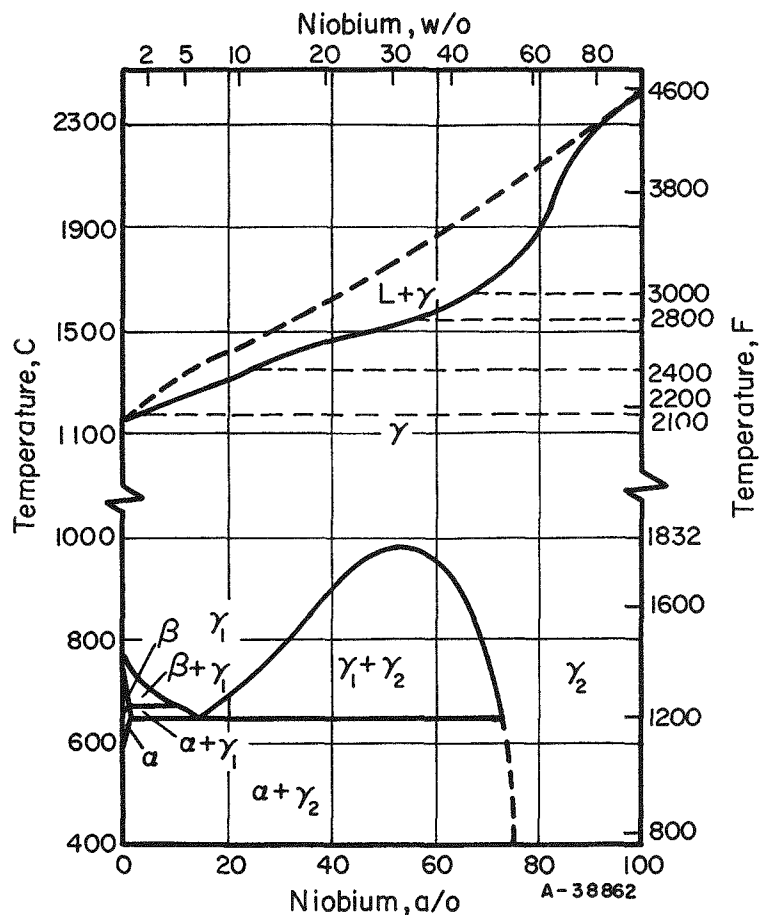


FIGURE 3. NIOBIUM-URANIUM PHASE DIAGRAM

Dashed lines show temperature of fabrication and points where segregation could cause localized melting.<sup>(3)</sup>

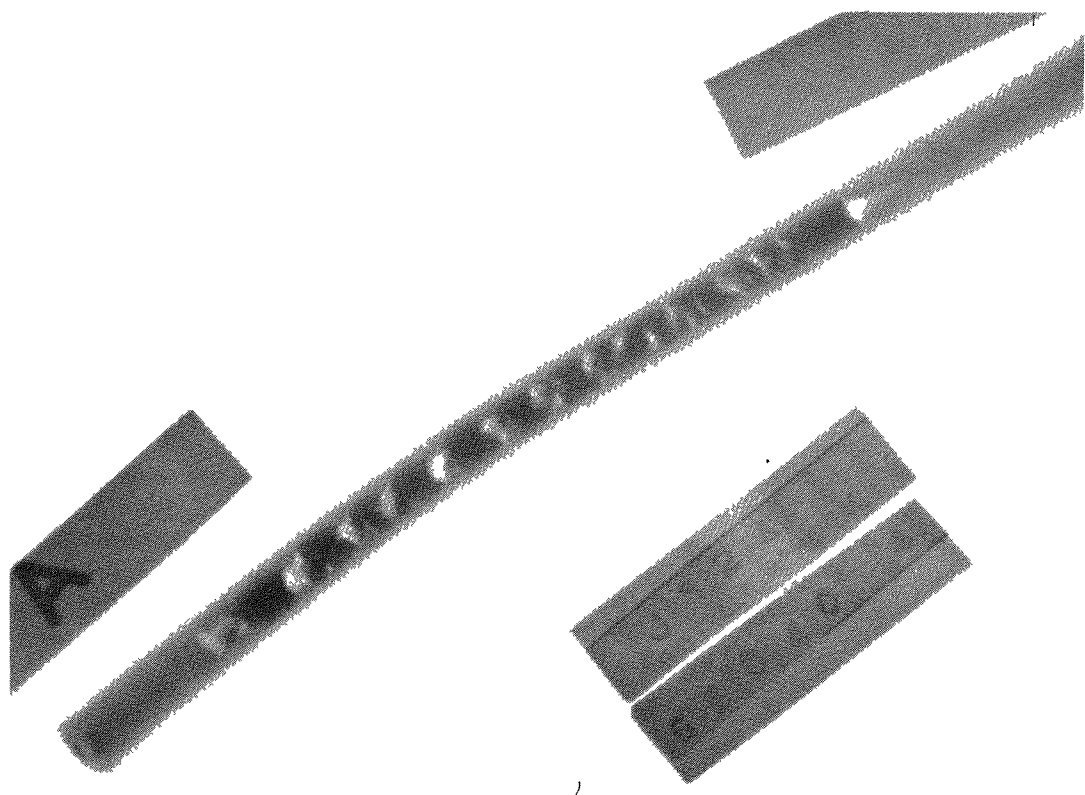


FIGURE 4. RADIOGRAPH OF NIOBIUM-30 w/o URANIUM  
ALLOY ROD ROLLED AT 2400 F

prepared by means of consumable-electrode melting into a skull prior to pouring into a copper mold. Although microsegregation in niobium-uranium ingots with greater than 20 w/o uranium appears to be inherent in a cast product, it was felt that the macro-segregation or banding might be eliminated by skull-melting procedures since arc-current fluctuations while the metal is solidifying, as in conventional cold-mold arc melting, would not be present. In addition, past experience with skull melting and casting of other alloys has revealed that the grain size of the cast product is reduced as compared with that observed in conventional cold-mold arc-melted material. It was anticipated that this reduced grain size, if obtained, would further facilitate subsequent fabrication.

#### Melting Studies

The starting materials consisted of a center-cut biscuit uranium having a nominal analysis of 30 ppm oxygen and 2 ppm hydrogen and niobium sintered bar (Table 3).

In order to build up a skull of sufficient height and thickness to allow for adequate molten metal to fill the mold, a lower grade of niobium (containing approximately 500 ppm oxygen) was used. Three electrodes of approximately 8 lb each of this unalloyed niobium were consumably melted into the water-cooled copper skull under a vacuum. After the last of these melts, an experimental ingot was poured to obtain a cavity in the skull of sufficient depth to allow for adequate molten metal to fill the mold. (Some metal will remain as solid in the skull due to heat losses to the water-cooled crucible.) This mold (Figure 5) consisted of three stepwise sections having the dimensions 3 by 4 by 1 in., 3 by 2 by 1/2 in., and 3 by 2 by 1/4 in. The mold cavity was adequately filled and a cursory examination of the resultant ingot revealed a very good surface.

The electrodes prepared for consumable-electrode arc melting into the skull prepared above consisted of 3/4-in.-square niobium bar with appropriately weighed uranium strips welded to opposite sides of the electrode. Uranium strips of the proper dimensions were pickled and fusion welded to the niobium in an inert atmosphere. Two electrodes of this type were welded together edgewise so as to give a final electrode with a cross section of approximately 1-1/2 by 3/4 (plus appropriate uranium width) in. Each electrode then contained approximately 100 per cent overcharge of material required to fill the mold. The electrode configuration can be seen in Figures 6 and 7 which illustrate the skull-melting setup.

All ingots were melted under vacuum utilizing from 3000 to 3500-amp arc current, and were cast into the water-cooled copper mold. The unalloyed niobium was melted first followed by melts of increasing uranium content. A tabulation of the cast ingot sizes can be found in Table 6.

Recovery (i.e., weight of ingot/weight of electrode) was adequate in all cases except for the two unalloyed niobium ingots. As referenced in Table 6, two unalloyed niobium ingots were poured. The recovery for each of these was only 12 per cent compared with a recovery of greater than 50 per cent with all alloyed ingots. The cause of this poor recovery is not known. Factors which can influence recovery include: skull- and electrode-alloy melting points, the starting weight of the skull, and the position and the fit of the skull in the copper crucible.

As can be seen from the chemical analysis of the resultant ingots (Table 7) the uranium content in all alloys was lower than that desired. It appears that some remelting

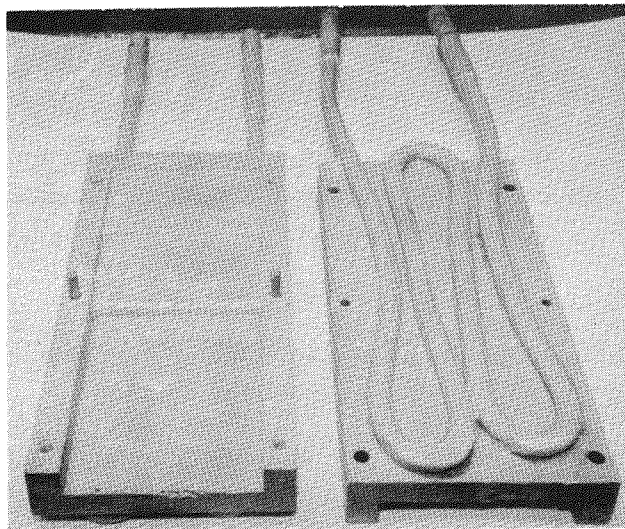


FIGURE 5. WATER-COOLED COPPER STEP MOLD

Mold size, top to bottom:

3 by 1/4 by 2 in.

3 by 1/2 by 2 in.

3 by 1 by 4 in.

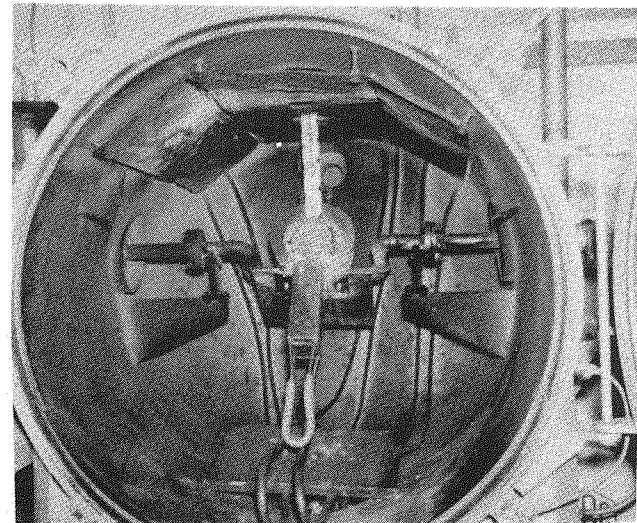


FIGURE 6. SKULL-MELTING-FURNACE SETUP  
SHOWING VACUUM CHAMBER

Electrode is in position with crucible  
tipped for pouring.

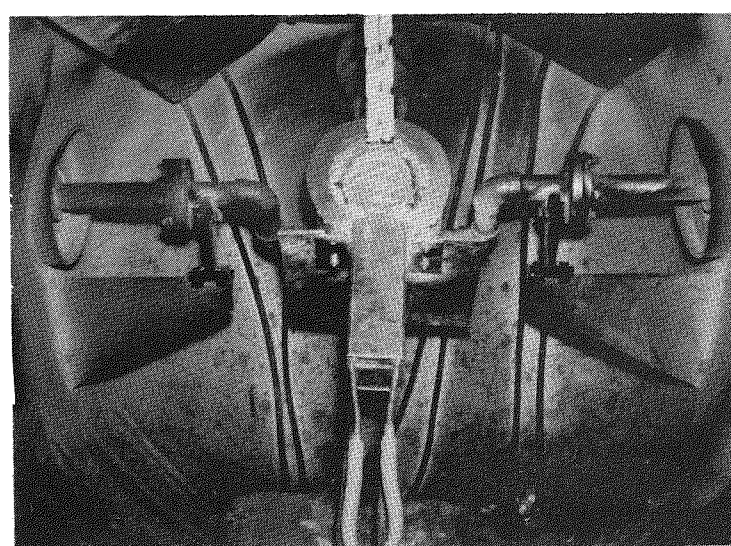


FIGURE 7. VIEW OF FURNACE INTERIOR SHOWING  
SKULL BUILDUP IN CRUCIBLE

TABLE 6. SIZE OF EACH NIOBIUM-URANIUM INGOT CAST UTILIZING CONSUMABLE-ELECTRODE SKULL-MELTING TECHNIQUES

Ingot	Nominal Composition (Balance Niobium), w/o	Ingot Size(a)
Nb-X	Unalloyed Nb(b)	3 by 1 by 1-1/4 in. 3 by 1 by 1-1/4 in.
A	10 U	3 by 1 by 4 in. 3 by 1/2 by 2 in. 3 by 1/4 by 2 in.
B	20 U	3 by 1 by 4 in. 3 by 1/2 by 2 in.
C	30 U	3 by 1 by 4 in. 3 by 1/2 by 2 in. 3 by 1/4 by 2 in.
D	40 U <sup>(b)</sup>	3 by 1 by 4 in.
E	50 U	3 by 1 by 4 in. 3 by 1/2 by 2 in. 3 by 1/4 by 2 in.

(a) All slabs of the same composition were cast in the same ingot utilizing a mold of stepwise configuration with the exception of unalloyed niobium slabs which were cast independently.

(b) Attempted to cast only larger section (3 by 1 by 4 in.) of mold.

TABLE 7. ANALYSIS OF SKULL-MELTED NIOBIUM-URANIUM INGOTS

Ingot	Uranium Content, w/o		Hydrogen, ppm	Oxygen, ppm
	Nominal	Analyzed		
A	10	4.38	3	160
B	20	14.3	--	--
C	30	25.0	--	--
D	40	34.6	--	--
E	50	46.7	2	115

of the residual skull, which was lower alloy content, occurred in each case, thereby lowering the uranium content below that desired. This occurrence is the reverse of that observed in melting the two unalloyed niobium charges where a great percentage of the charge material was not recovered but froze onto the existing skull. The decreasing melting point of niobium with increasing uranium content may, in part, explain this behavior. In addition, the skull was removed after each melt to facilitate positioning of the next electrode to be melted. Due to slight variations in the contour of the outside surface of the skull, the heat-transfer coefficient across the skull-crucible interface could be altered sufficiently to have a significant effect on the rate of cooling in the skull.

The oxygen pickup upon melting appears to be very small as indicated in Table 7. Analyses were made on one of the first ingots cast as well as the last ingot cast with the resultant analyses in the same range. Oxygen contamination from the niobium skull was minor as was expected.

Ingots containing 34.6 and 46.7 w/o uranium both cracked upon solidification. The fracture interface shows an area of very porous material, most probably a result of shrinkage. (See Figure 8). These alloys apparently could not withstand the thermal shock imparted by chilling on the water-cooled copper mold.

A photograph of all of the ingots cast is shown in Figure 9. The Nb-X ingot was cast during the skull buildup and was subsequently used as a mold plug for casting the single-mold section of unalloyed niobium and niobium-40 w/o uranium ingots.

The microstructures shown in Figure 10 of selected compositions appear very similar to those cast by the conventional cold-mold consumable-electrode arc-melting technique.<sup>(1)</sup> Segregation on a microscale is present, the dark dendrites being rich in uranium.

Radiographs of the 3 by 1 by 4-in. section of the as-cast ingots (see Figure 11) revealed quite a bit of shrinkage porosity. However, there is no evidence of macrosegregation or banding. For purposes of comparison, Figure 12, a radiograph, shows a banding in a niobium-30 w/o uranium ingot cast by the conventional cold-mold arc-melting technique.

Although further development of skull-melting procedures for the production of sound niobium-uranium alloys is required, it has been shown that macrosegregation can be eliminated by skull melting and casting. Microsegregation, however, is not eliminated by these techniques.

#### FABRICATION STUDIES OF SKULL-CAST ALLOYS

Flat rolling was the only fabrication method employed for the skull-cast slabs. The 1/2- and 1/4-in. -thick slabs were utilized in this study.

Initially, the 1/4-in. -thick slabs were rolled in air at 1000 F. Both the niobium-25.0 and -46.7 w/o uranium alloy showed edge cracking after very slight reductions in thickness and the rolling temperature was raised to 1850 F. At this temperature, the

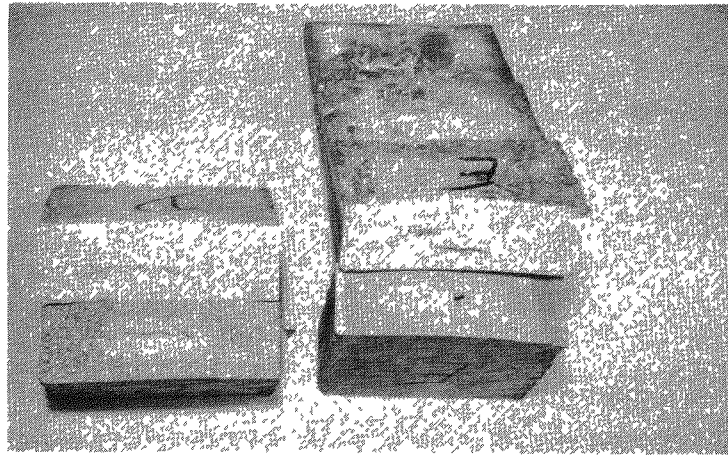


FIGURE 8. FRACTURED SURFACES OF INGOTS CONTAINING  
34.6 w/o URANIUM (INGOT D) AND 46.7 w/o  
URANIUM (INGOT E)

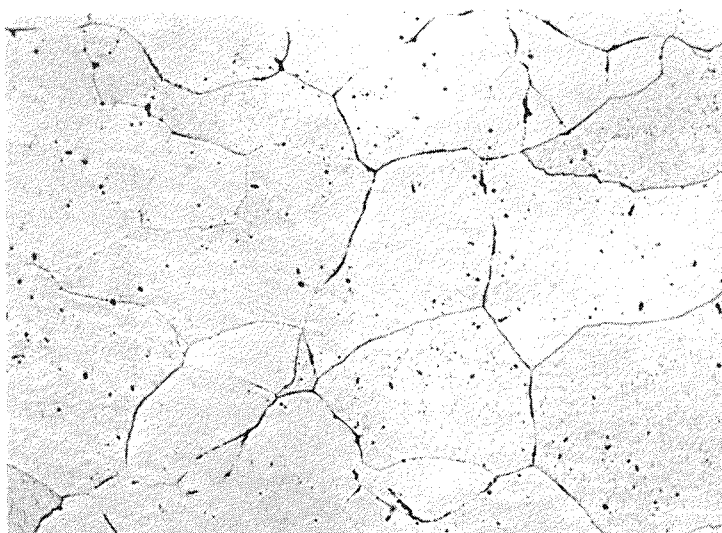
The fractured interfaces show areas of porous  
material which probably is due to shrinkage.



FIGURE 9. SKULL-MELTED NIOBIUM-URANIUM INGOTS

Identification:

Nb-X	- unalloyed niobium	C	- niobium-25.0 w/o uranium
A	- niobium-4.38 w/o uranium	D	- niobium-34.6 w/o uranium
B	- niobium-14.3 w/o uranium	E	- niobium-46.7 w/o uranium

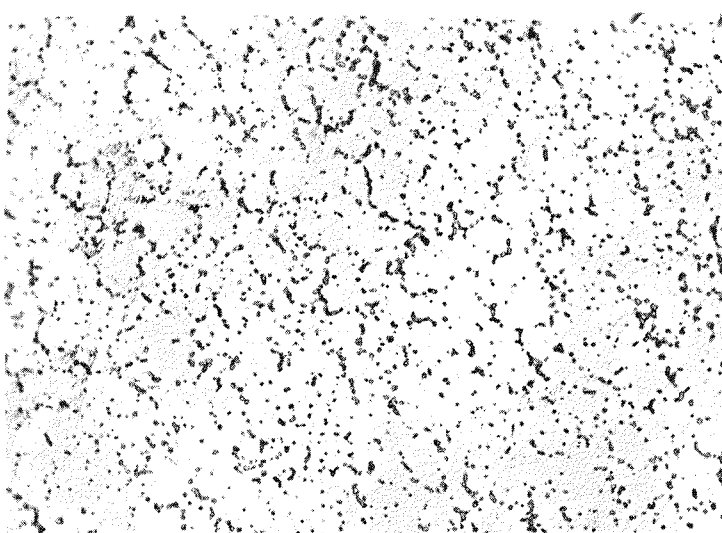


100X

RM18355

## a. Niobium-4.38 w/o Uranium

Slight grain-boundary segregation is evident.

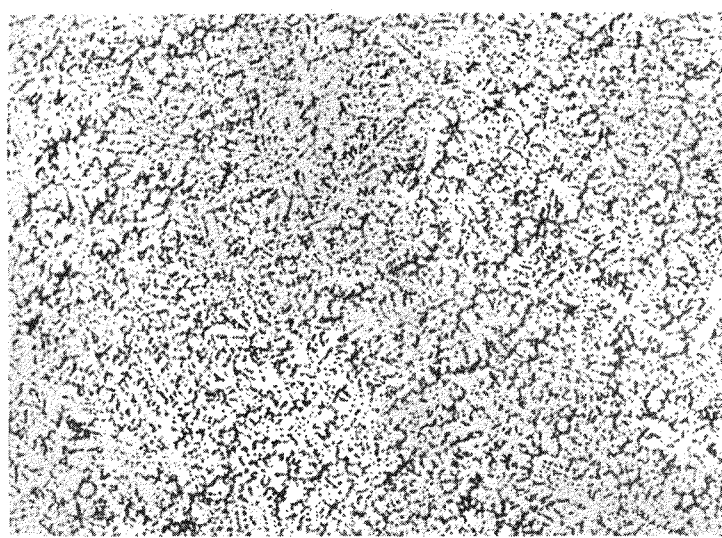


100X

RM18359

## b. Niobium-25.0 w/o Uranium

Note dendritic, cored structure.



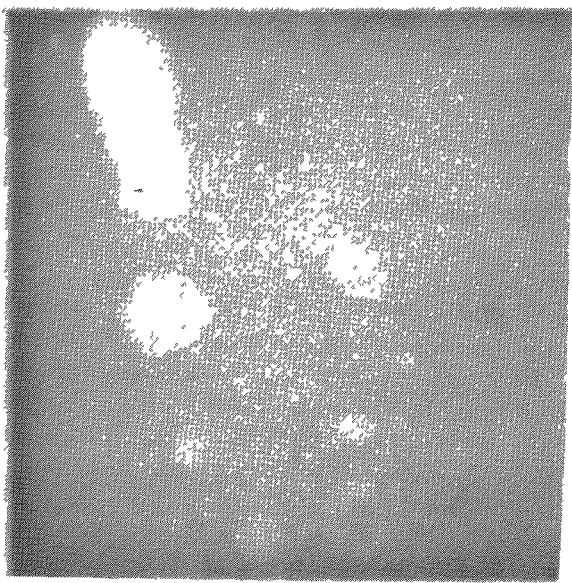
100X

RM18361

## c. Niobium-46.7 w/o Uranium

Two-phase structure is shown.

FIGURE 10. MICROSTRUCTURES OF SKULL-MELTED NIOBIUM-URANIUM ALLOYS



a. Niobium-4.38 w/o Uranium, Ingot A



b. Niobium-25.0 w/o Uranium, Ingot C

FIGURE 11. RADIOPHGRAPHS OF NIOBIUM-URANIUM INGOTS

Extensive shrinkage is evident. No macrosegregation or banding is visible.

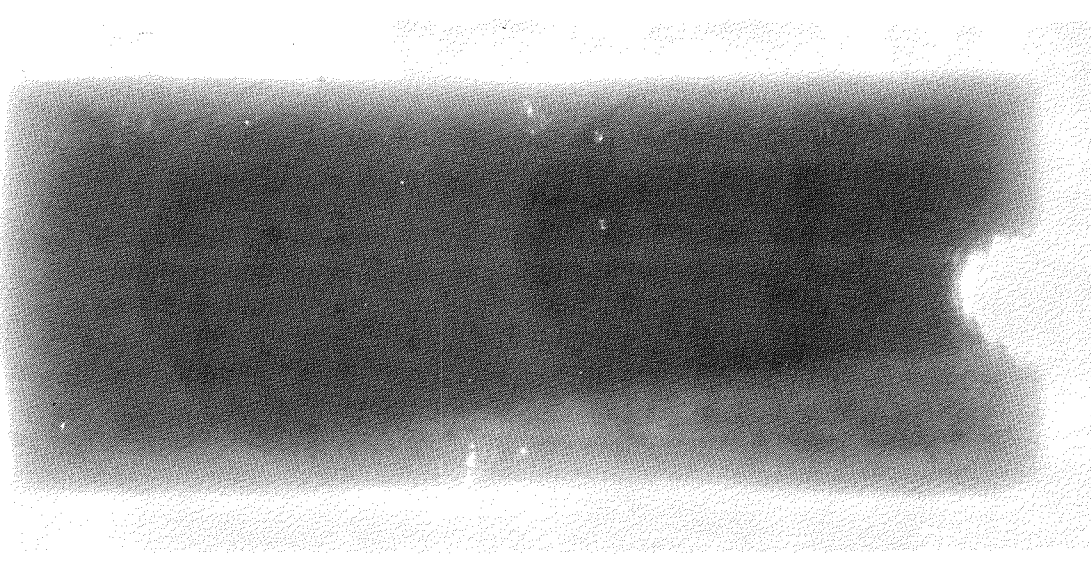


FIGURE 12. RADIOGRAPH SHOWING MACROSEGREGATION OR BANDING  
IN A NIOBIUM-30 w/o URANIUM ALLOY CAST BY THE  
CONVENTIONAL CONSUMABLE-ELECTRODE ARC-MELTING  
TECHNIQUE

niobium-25.0 w/o uranium alloy was reduced with some edge and surface cracking but fabrication of the niobium-46.7 w/o uranium alloy was unsuccessful. These results are summarized in Table 8. Figure 13 shows macrographs of the fabricated sheet. The fabricability of the 4.38 and 14.3 w/o uranium alloys produced by skull casting appears to be better than that experienced with consumable-electrode arc castings. This was the first material whose cast structure could be broken down by direct rolling without initial forging. This improvement is probably due to ingot geometry since little evidence of grain refinement was noted. Fabrication of the niobium-25.0 w/o uranium alloy is at best marginal at 1850 F, while the niobium-46.7 w/o uranium alloy was not fabricable at either 1000 or 1850 F.

TABLE 8. FABRICATION RESULTS WITH SKULL-CAST NIOBIUM-URANIUM ALLOYS

Composition (Balance Niobium), w/o	Temperature, F	Reduction in Thickness, per cent	Remarks
4.38 U	1000	80	Sound sheet, slight edge cracking
14.3 U	1000	80	Ditto
25.0 U	1000	10	Edge cracking; temperature raised for subsequent fabrication
	1850	84(a)	Edge and surface cracking; material is marginal
46.7 U	1000	1	Severe edge cracking; temperature raised
	1850	19(a)	Specimen fractured

(a) Per cent reduction includes that obtained at 1000 F.

A 1/2-in.-thick section of the niobium-46.7 w/o uranium alloy was sectioned into 3 by 1/2-in. pieces. These samples were encased in a molybdenum can (Figure 1) and flat rolled at 2000, 2200, 2400, and 2500 F. All of the specimens were reduced approximately 85 per cent but exhibited extensive cracking generally completely across the sheet perpendicular to the rolling direction. No successfully fabricated material was obtained.

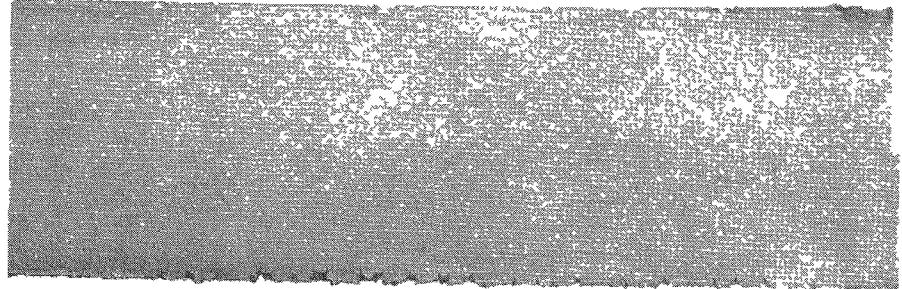
Although improvement in the fabricability of the lower-uranium-containing alloys was observed, skull-melted material containing higher amounts of uranium (above 25 w/o) did not appear to be any more fabricable than alloys cast by the conventional consumable-electrode arc-melting technique.



1X

RM18036

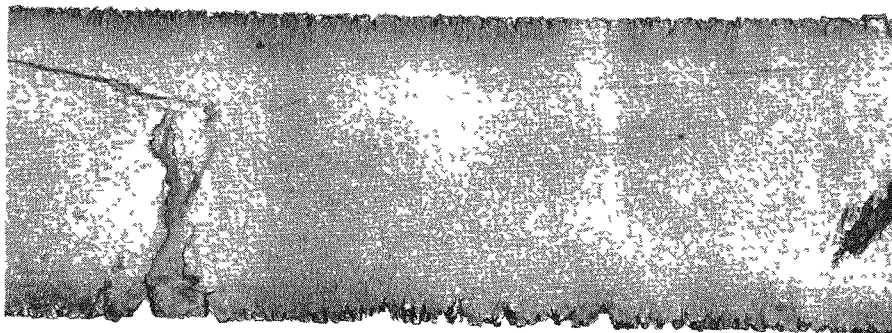
a. Niobium-4.38 w/o Uranium Alloy Reduced 80 Per Cent by Rolling at 1000 F



1X

RM18037

b. Niobium-14.3 w/o Uranium Alloy Reduced 80 Per Cent by Rolling at 1000 F



1X

RM18038

c. Niobium-30 w/o Uranium Alloy Reduced 84 Per Cent by Rolling at 1000 and 1850 F

1X

RM18039

d. Niobium-46.7 w/o Uranium Alloy Specimen That Failed to Roll at 1850 F



21

FIGURE 13. FLAT-ROLLED SKULL-CAST NIOBIUM-URANIUM ALLOYS

MECHANICAL-PROPERTY DETERMINATIONS

Tensile strength and creep data for the niobium-4.38, -10, -14.3, and -20 w/o uranium alloys were obtained at elevated temperatures. These mechanical-property data are of interest both from the viewpoint of structural design and in predicting irradiation swelling. The data presented in this section were obtained on material prepared both by skull-melting and by consumable-electrode arc-melting techniques. All specimens were given a 1-hr vacuum stress-relief anneal at 1800 F prior to testing.

Elevated-Temperature Short-Time  
Tensile Tests

Elevated-temperature tensile tests were performed on niobium-uranium alloy sheet specimens in vacuum testing units. Stress-strain curves for temperatures below 1800 F were obtained with a mechanical extensometer. A deflectometer, which measured crosshead movement, was used to obtain stress-strain curves for specimens tested above 1800 F.

Figure 14 shows plots of the tensile strengths of the niobium-uranium alloys versus temperature. The alloys shown retained their strengths well even above 2000 F. In Figure 15, the ultimate tensile strength of the niobium-uranium alloys tested is compared with that of unalloyed niobium and niobium-2.37 w/o chromium(5) a high-strength, niobium-base alloy. The niobium-uranium alloys compare quite favorably. Uranium appears to be a potent strengthener of niobium. However, from Figure 16, which is a plot of tensile strength versus uranium content, it is apparent that after the initial increase in strength further increases in strength due to increasing uranium content are relatively small. The main benefit derived from uranium content above 4 w/o is from increased fuel loading.

Tensile tests performed on the niobium-10 w/o uranium alloy material produced apparent discrepancies in strength at 1600 F. The ultimate tensile strength of the initial alloy specimen tested was much higher than expected. Further tensile tests above 1600 F indicated that its strength was as high as that of the niobium-20 w/o uranium alloy. The tensile ductility of this niobium-10 w/o uranium alloy was quite low, however (1 per cent), compared with that of the niobium-20 w/o uranium alloy (10 per cent). Analyses of the wrought sheet from the three heats of the niobium-10 w/o uranium alloy being tested showed large differences in oxygen content. The oxygen content of the three heats was 680, 1190, and 3170 ppm. A plot of oxygen content versus ultimate tensile strength is shown in Figure 17 for niobium-10 w/o uranium alloys tested at 1600 F. As can be seen, the tensile strength seems to increase linearly with increasing oxygen content while the tensile elongation drops rapidly. Since it is generally believed that the strengthening effect due to oxygen content decreases with increasing temperature, a more thorough investigation of the strength of the niobium-10 w/o uranium alloy containing 3170 ppm oxygen was made at temperatures up to 2200 F. A plot of the tensile strength of the niobium-10 w/o uranium -0.31 w/o oxygen alloy as a function of temperature is found in Figure 18. The data presented show that the niobium-10 w/o uranium -0.31 w/o oxygen alloy is extremely brittle in the temperature range between 800 and 1500 F. All specimens tested in the abovementioned temperature range failed while the material was still undergoing elastic deformation. These values are plotted as fracture

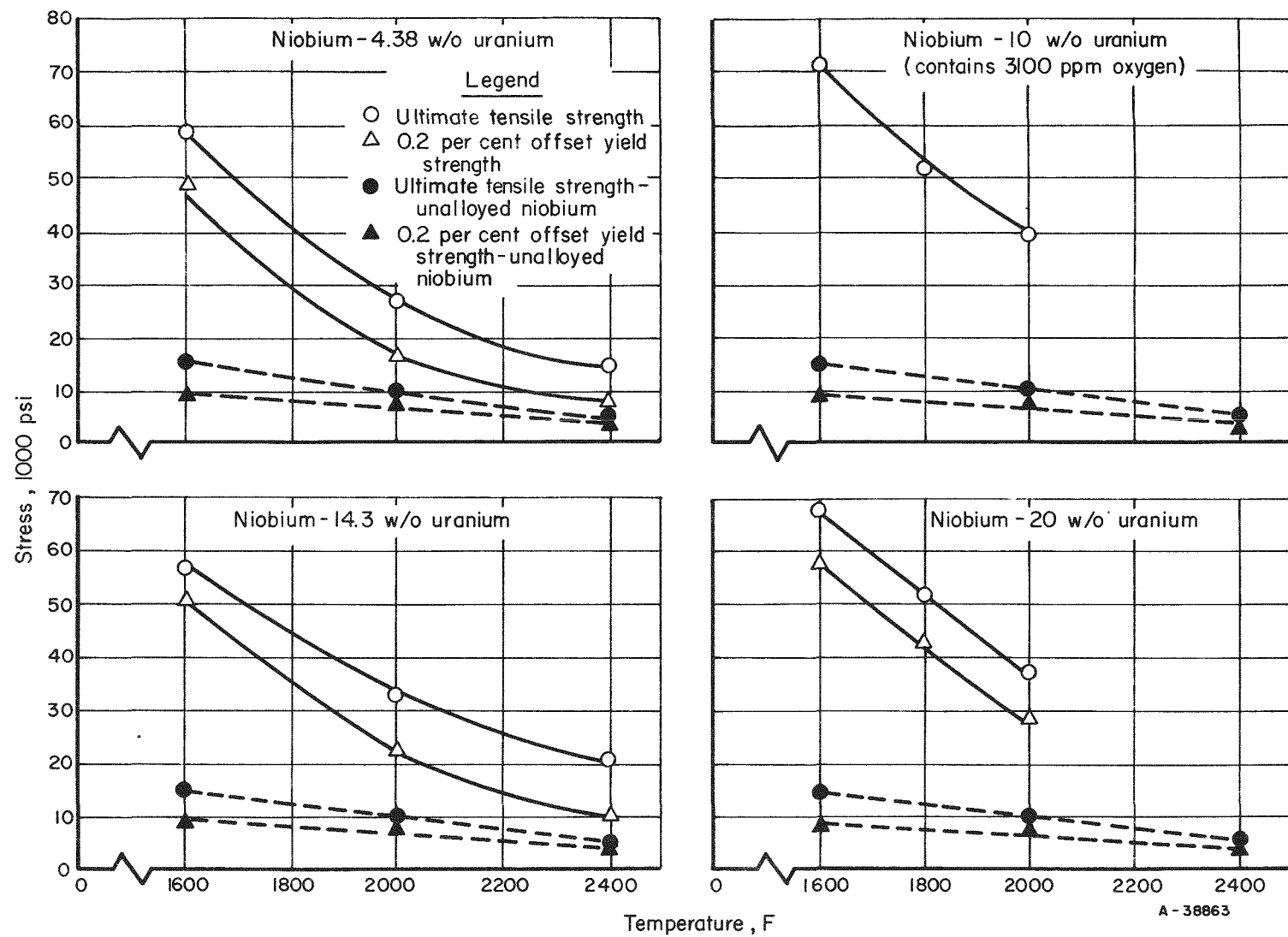


FIGURE 14. EFFECT OF TEMPERATURE ON THE TENSILE STRENGTH OF NIOBIUM-URANIUM ALLOYS AND UNALLOYED NIOBIUM

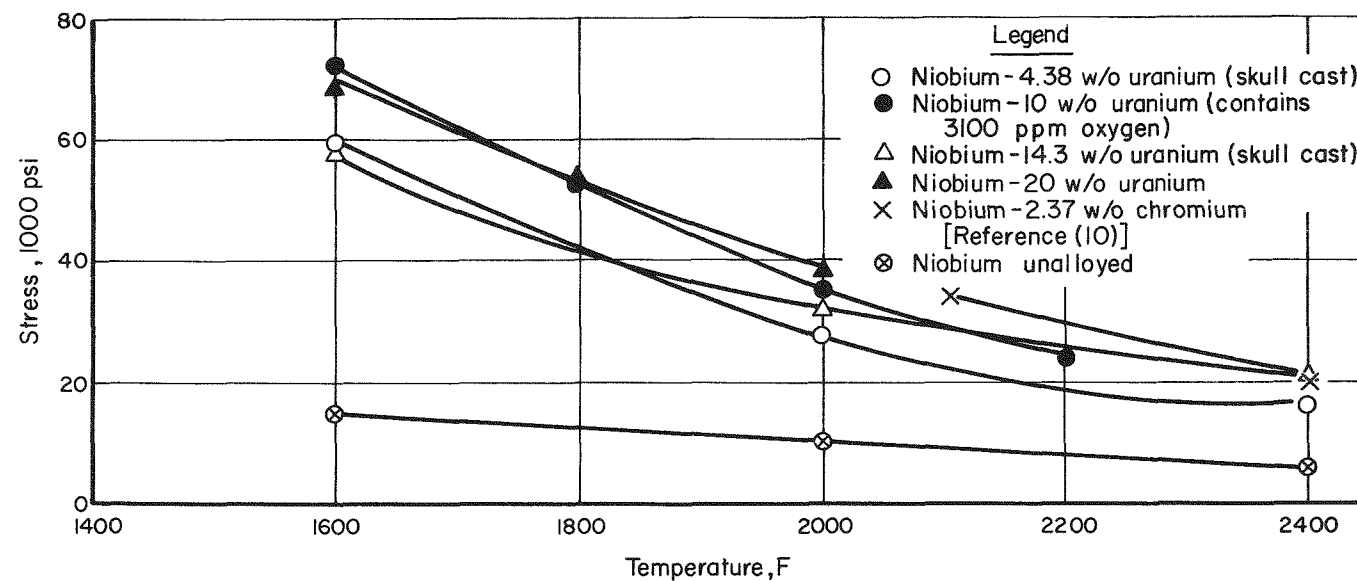


FIGURE 15. COMPARISON OF ELEVATED-TEMPERATURE ULTIMATE TENSILE STRENGTH OF CONSUMABLE-ELECTRODE ARC-MELTED AND SKULL-CAST NIOBIUM-URANIUM ALLOYS

24

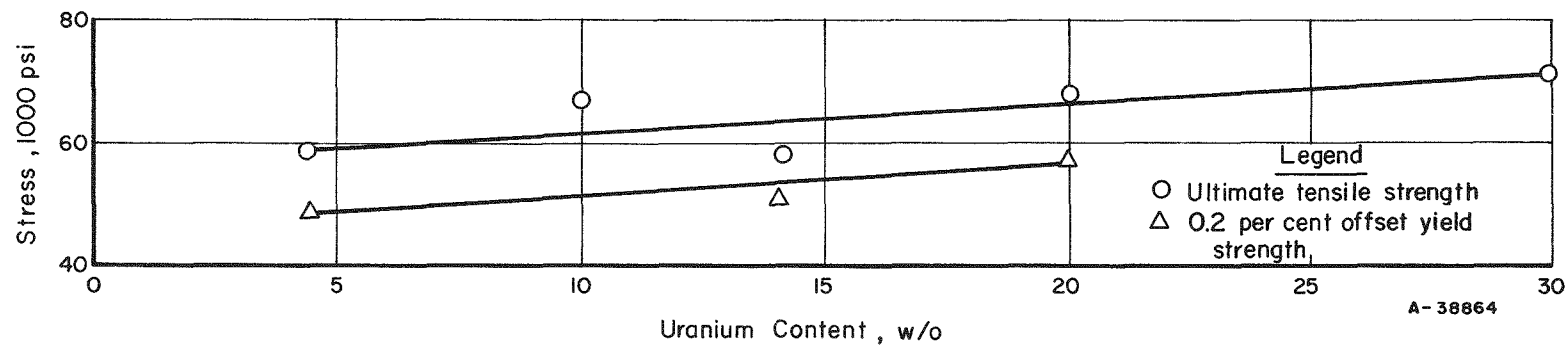


FIGURE 16. EFFECT OF INCREASING URANIUM CONTENT ON THE TENSILE STRENGTH OF NIOBIUM-BASE ALLOYS AT 1600 F

A-38864

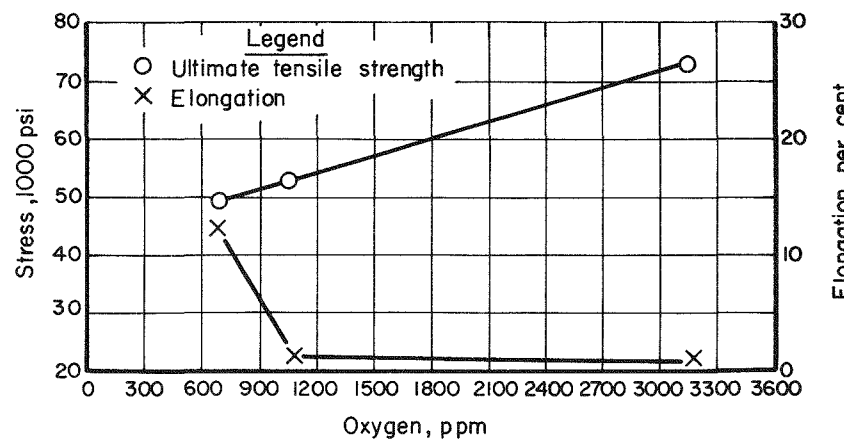


FIGURE 17. EFFECT OF INCREASING OXYGEN CONTENT ON ULTIMATE TENSILE STRENGTH AND ELONGATION OF NIOBIUM-10w/o URANIUM ALLOY AT 1600 F

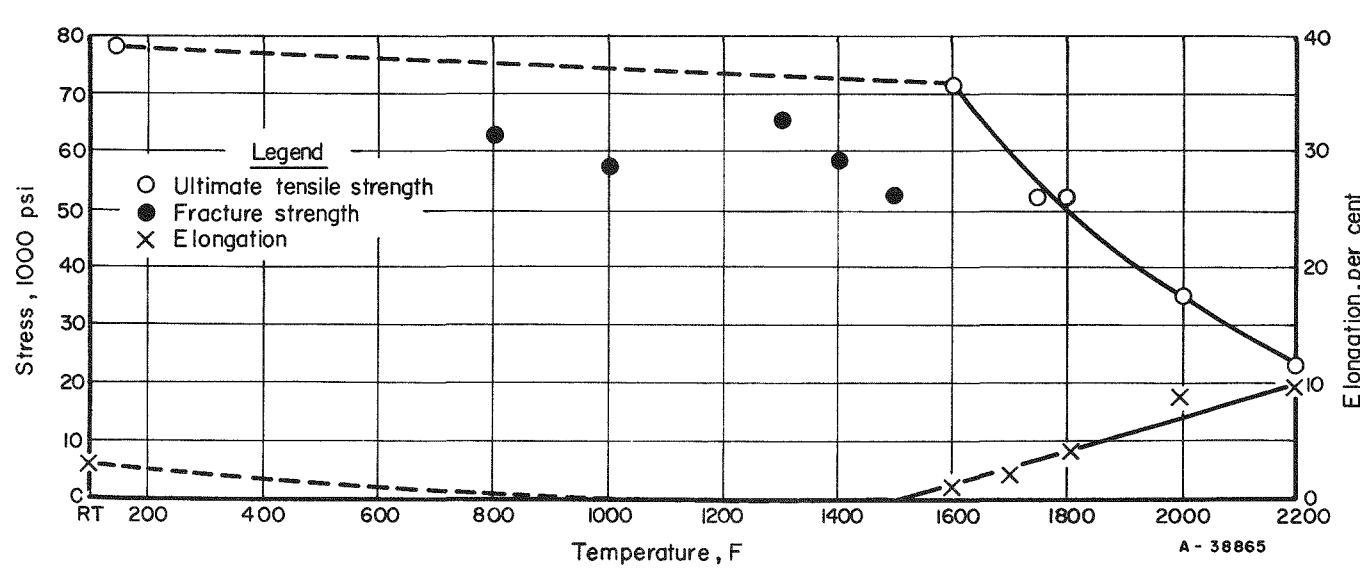


FIGURE 18. EFFECT OF TEMPERATURE ON TENSILE PROPERTIES OF NIOBIUM-10 w/o URANIUM ALLOY CONTAINING 3100 PPM OXYGEN

strengths in Figure 18. Above 1500 F some ductility was noted and the material underwent plastic deformation. Ductility as measured by tensile elongation was low (10 per cent) even at 2200 F where elongations on the order of 80 to 90 per cent could be expected for low-oxygen material.

The effect of oxygen on niobium-10 w/o uranium alloys is important in that it indicates that although 0.3 w/o oxygen is an effective strengthener of niobium at elevated temperature, the high-oxygen content results in a severe reduction in ductility, which is generally undesirable.

The niobium-uranium alloys possess rather remarkable strength at temperatures up to 2000 F. A glance at Table 9, which compares the tensile strength of the niobium-uranium alloys with that of several commonly used high-strength alloys, shows that the niobium-uranium alloys are as strong or stronger than any alloy listed at 1800 F and also exhibit comparable ductility. This high strength at elevated temperature negates the need for a cladding material which must support the fuel core. The niobium-uranium alloys appear to need a cladding which will primarily protect them from the coolant and reduce the hazard of radioactive contamination of the coolant.

### Creep Studies

The stresses which result in minimum creep rates of 0.001, 0.01, and 0.1 per cent per hr were determined at 1600 and 2000 F for the niobium-4.38 and 14.3 w/o uranium alloys and at 1600 and 1800 F for the niobium-10 and -20 w/o uranium alloys. All creep tests were performed in standard creep machines. Vacuum was maintained at about  $5 \times 10^{-4}$  mm of mercury and temperatures were controlled to about  $\pm 5$  F for each test. A filar microscope was used to measure creep deformation. Results are shown in Table 10 and are plotted in Figures 19 and 20.

In Figure 20, the creep rates for all four alloys tested are compared. As can be seen, all four alloys follow the same general slope at 1600 F. The niobium-10 w/o uranium alloy follows the same general slope even though it had been strengthened additionally through accidental contamination by oxygen as well as the addition of uranium.

A summary of the stresses that will produce creep rates of 0.001, 0.01, and 0.1 per cent per hour is shown in Table 11.

Design curves for the niobium-4.38 and -14.3 w/o uranium alloys are presented in Figures 21 and 22. These figures show rupture curves and also curves representing various percentages of total deformation as related to specific stresses and times of application. Curves were not prepared for the niobium-10 and -20 w/o uranium alloys as data for these alloys were not complete.

The creep strength obtained for the niobium-10 w/o uranium alloy is higher than expected, this is undoubtedly due to the high oxygen content of this alloy as discussed in the previous section. Chemical analyses of the niobium-4.38 w/o uranium alloy indicate that 1100 ppm oxygen is present in this alloy which probably explains why its creep strength is higher than that of either the niobium-14.3 (contains 160 ppm oxygen) or -20 w/o (contains 198 ppm oxygen) uranium alloy. Contamination of the niobium-4.38 and -10 w/o uranium alloy creep specimens with oxygen probably occurred during vacuum stress-relief annealing.

TABLE 9. COMPARISON OF SHORT-TIME TENSILE PROPERTIES OF NIOBIUM-URANIUM ALLOYS AND SELECTED STRUCTURAL MATERIALS

Material	Temperature, F	0.2 Per Cent Offset Yield Strength, psi	Ultimate Tensile Strength, psi	Elongation, per cent	Reference
Nb-4.38 w/o U	1600	49,850	58,940	9.0	--
	2000	16,880	27,420	2.5	--
	2400	8,500	15,600	6.6	--
Nb-10 w/o U	1600	--	72,000	1	--
	1800	44,600	52,500	4.0	--
	2000	25,400	35,300	9.0	--
	2200	--	24,000	10.0	--
Nb-14.3 w/o U	1600	50,970	57,060	14.0	--
	2000	22,370	32,870	57.0	--
	2400	10,200	21,100	66.0	--
Nb-20 w/o U	75	93,200	102,000	7	(1)
	1600	58,100	68,400	10	(1)
	1800	43,000	52,000	34	--
	2000	28,600	37,500	74	--
Unalloyed niobium	75	36,000	48,000	48	(6)
	1600	9,400	15,200	47	--
	2000	8,100	10,100	34	--
	2400	4,000	5,500	70	--
Type 304 stainless	75	34,000	85,000	63	(7)
	1500	10,000	21,000	39	--
	1900	--	7,000	63	--
Type 316 stainless	75	38,500	85,500	60	(7)
	1500	18,500	27,500	42	--
	1900	--	10,500	--	--
Hastelloy X	75	55,800	113,000	43	(8)
	1800	17,000	21,000	43	--
	2300	--	3,300	21	--
René 41	RT	140,000	185,000	20	(9)
	1650	75,000	75,000	12	--
	1800	35,000	35,000	20	--

TABLE 10. CREEP DATA ON NIOBIUM-BASE ALLOYS TESTED IN VACUUM

Alloy Composition (Balance Niobium), w/o	Temperature, F	Stress, psi	Rupture Time, hr	Initial Deformation, per cent	Deformation, per cent, After Indicated Time			Minimum Creep Rate, per cent per hr	Total Elongation, per cent
					10 Hr	100 Hr	500 Hr		
4.38 U	1600	35,000	41.4	0.396	2.48	--	--	0.175	16.5
		20,000	575.0 <sup>(a)</sup>	-0.010	0.235	0.735	4.77	0.005	5.75
14.3 U	1600	35,000	8.7	0.593	--	--	--	1.86	43.3
		30,000	17.5	-0.021	--	--	--	0.012	8.25
		20,000	337.6 <sup>(b)</sup>	0.161	1.05	3.94	--	0.029	13.9
		10,000	785.9 <sup>(c)</sup>	0.067	0.162	0.325	0.622	0.0007	0.778
4.38 U	2000	10,000	238.2	0.191	2.40	10.50	--	0.081	30.9
		5,000	145.1 <sup>(b)</sup>	0.182	0.450	0.745	--	0.002	0.807
14.3 U	2000	10,000	127.1	0.500	7.80	22.8	--	0.156	27.8
		5,000	11.0 <sup>(c)</sup>	0.075	--	--	--	0.15	2.2
		5,000	19.2 <sup>(d)</sup>	--	--	--	--	--	--
		4,000	157.4 <sup>(c)</sup>	0.043	0.42	0.92	--	0.0025	1.0
10 U	1600	30,000	60.2	--	--	--	--	0.71	1.0
		25,000	381.3	--	--	--	--	0.0052	6.0
		20,000	169.0 <sup>(b)</sup>	--	--	--	--	0.0028	0.8
	1800	20,000	28.9	--	--	--	--	0.036	14.0
		14,000	54.0	--	--	--	--	0.20	15.0
20 U	1600	30,000	38.7	--	--	--	--	0.71	82.7
		20,000	27.2	--	--	--	--	1.16	71.0
		15,000	169.7	--	--	--	--	0.122	93.0

(a) Test in progress.

(b) Test discontinued.

(c) Test failed due to flaw in material.

(d) Test discontinued, extensometer was not readable.

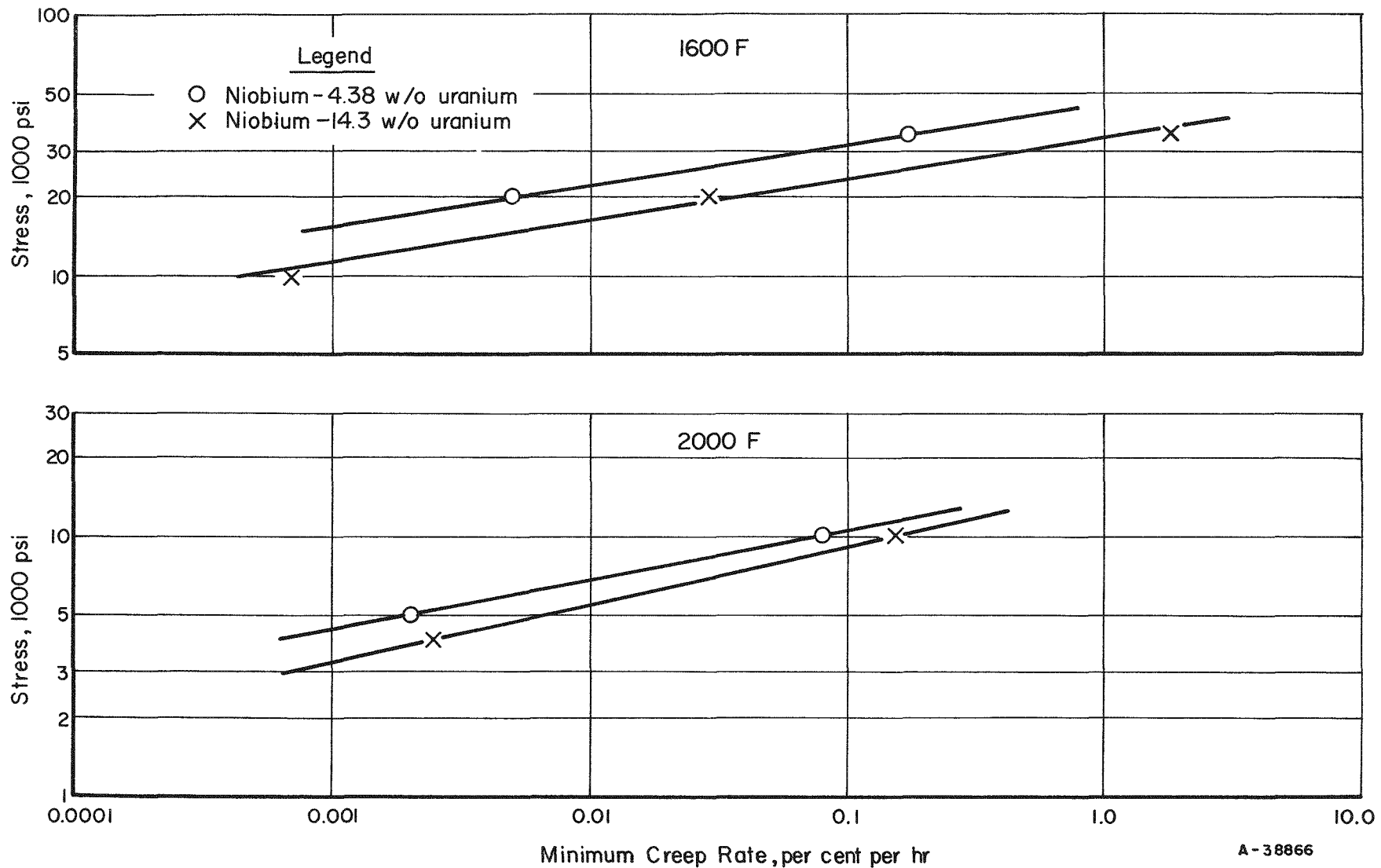


FIGURE 19. STRESS VERSUS MINIMUM CREEP RATE FOR TWO NIOBIUM-BASE ALLOYS AT 1600 AND 2000 F

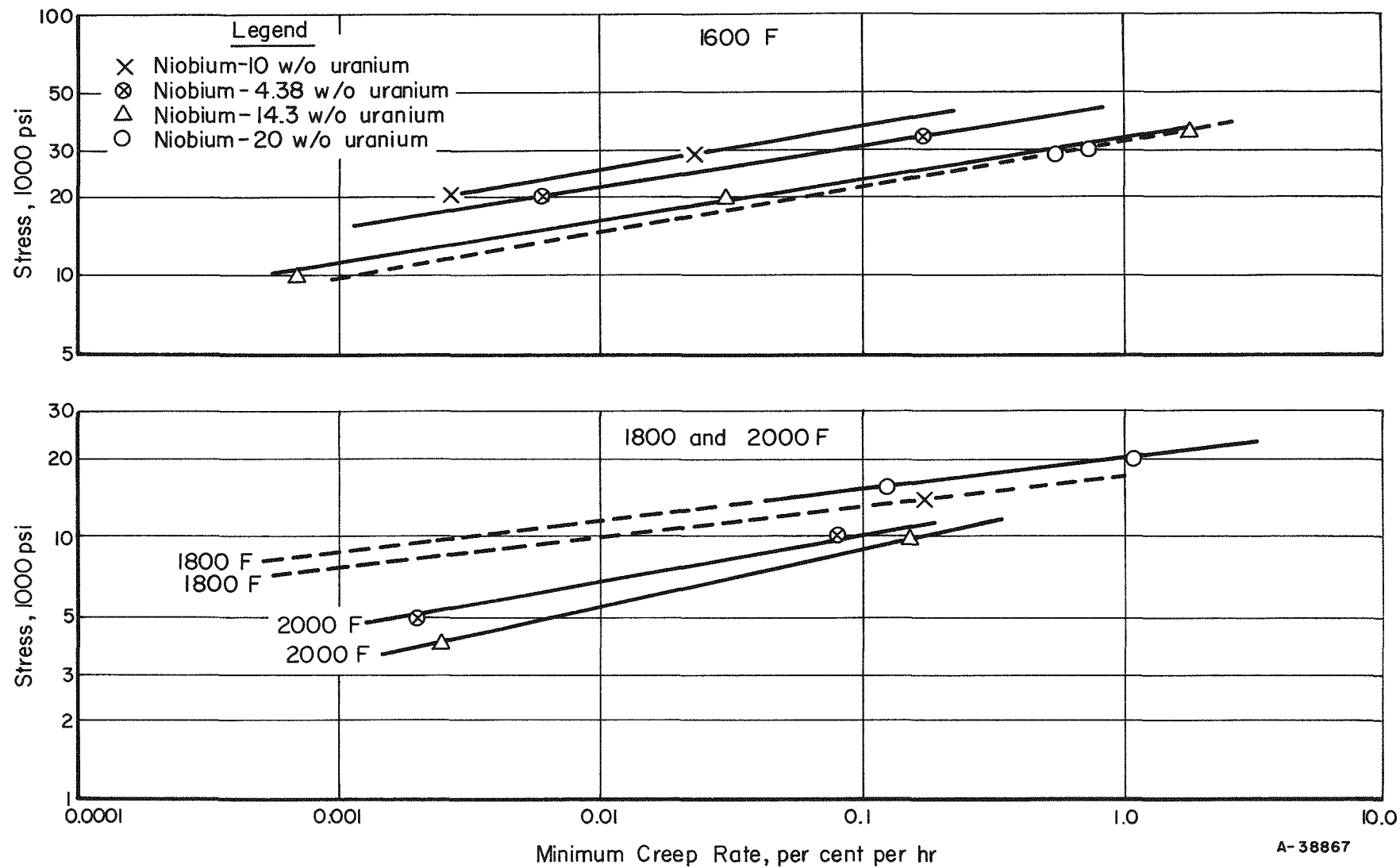


FIGURE 20. COMPARISON OF STRESS VERSUS MINIMUM CREEP RATES FOR FOUR NIOBIUM-URANIUM ALLOYS AT 1600, 1800, AND 2000 F

TABLE 11. STRESS TO PRODUCE CREEP RATES OF 0.001, 0.01, AND 0.1 PER CENT PER HR IN NIOBIUM-URANIUM ALLOYS

Alloy Composition (Balance Niobium), w/o	Stress, psi, to Produce Creep Rate Shown		
	0.001 Per Cent per Hr	0.01 Per Cent per Hr	0.1 Per Cent per Hr
<u>At 1600 F</u>			
4.38 U	15,000	22,000	31,500
10 U	17,000	25,000	37,000
14.3 U	11,000	16,000	23,500
20 U(a)	9,800	14,900	22,000
<u>At 1800 F</u>			
10 U	8,800	11,500	15,000
20 U(a)	7,800	10,000	13,000
<u>At 2000 F</u>			
4.38 U	4,400	6,800	10,500
14.3 U	3,300	5,400	9,000

(a) Stresses are estimated.

The data presented above indicate that the niobium-uranium alloys tested have creep strengths which are comparable to many structural materials. The strengths exhibited are more than sufficient for a fuel alloy and further indicate that a cladding material will be needed only to prevent corrosion and to contain fission products.

#### CORROSION-TEST RESULTS

Corrosion tests were performed to evaluate the behavior of niobium-uranium alloys in potential reactor coolants. The coolants studied were NaK at 1600 F, sodium at 1500 F, and water at 600 and 680 F.

#### In NaK and Sodium

Fabricated specimens of niobium-10 and -20 w/o uranium and as-cast specimens of niobium-30, -40, -50, and -60 w/o uranium were exposed to NaK at 1600 F and sodium at 1500 F. Testing was conducted in NaK because it is a commonly used heat-transfer medium in irradiation studies. Compatibility with sodium was determined since sodium is used as a reactor coolant. The experimental procedure was identical for testing in both media. Specimens were placed in stainless steel capsules which contained sufficient NaK (potassium-44 w/o sodium) or sodium to completely immerse the specimens.

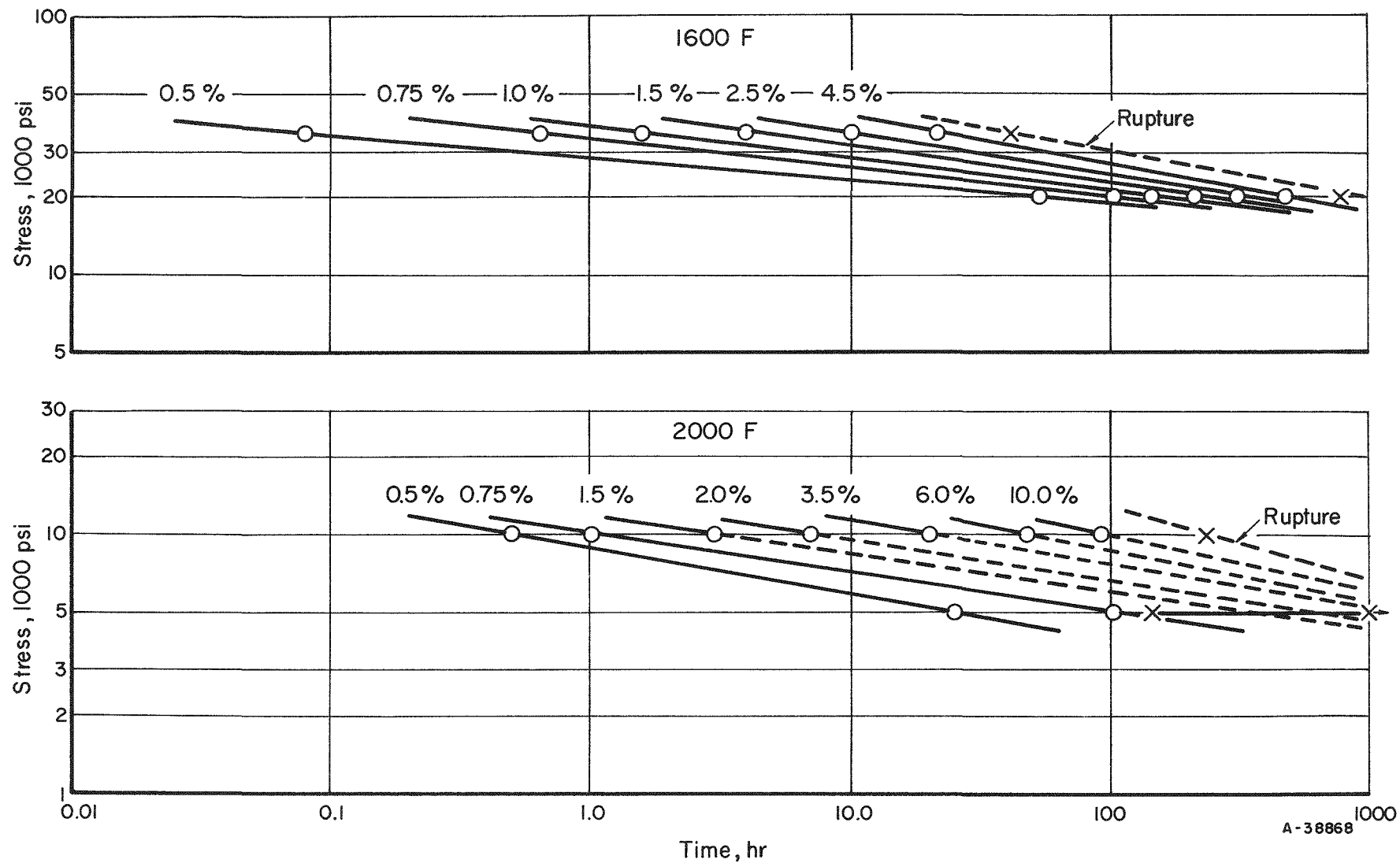


FIGURE 21. DESIGN CURVE FOR NIOBIUM-4.38 w/o URANIUM ALLOY AT 1600 AND 2000 F

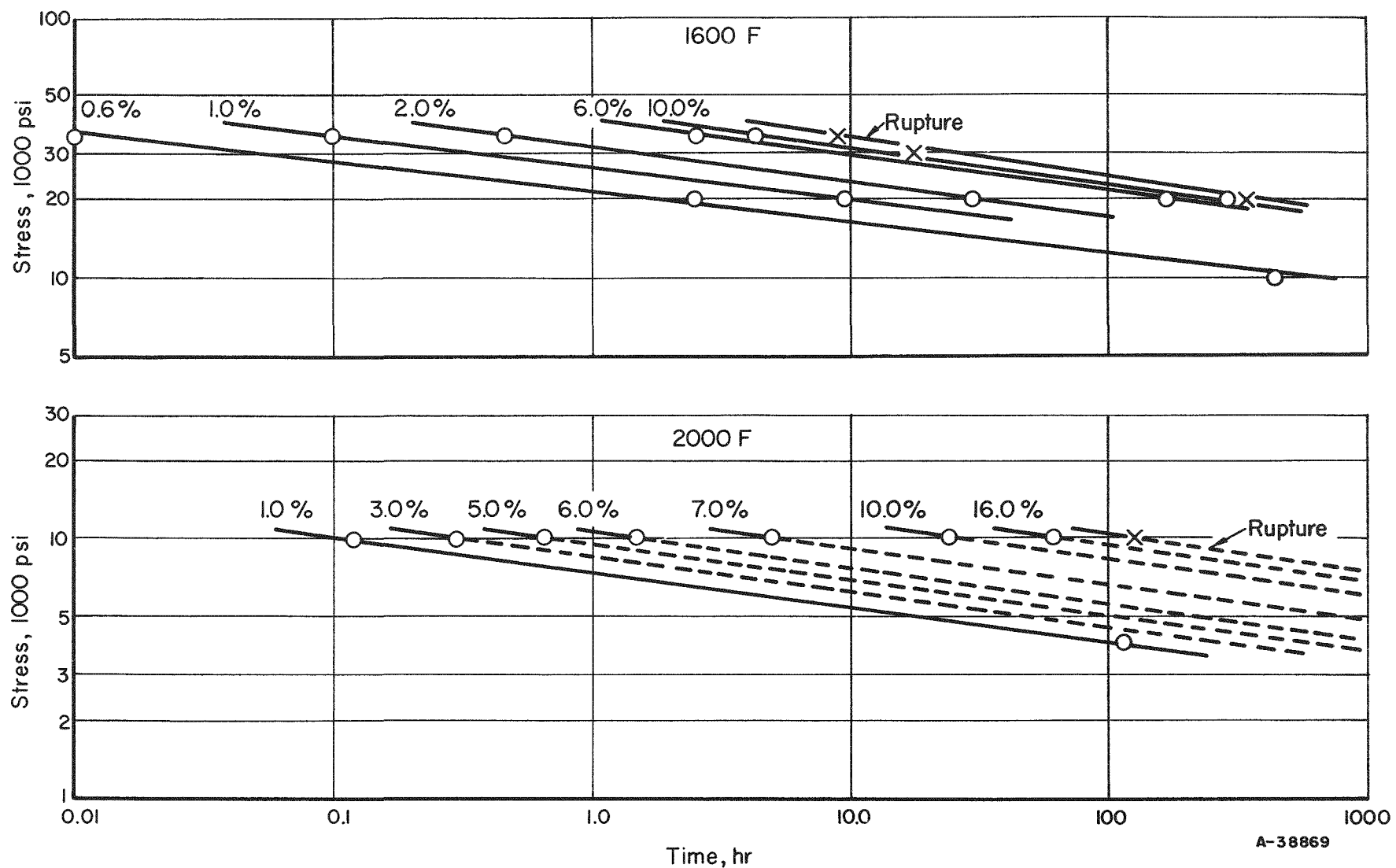


FIGURE 22. DESIGN CURVE FOR NIOBIUM-14.3 w/o URANIUM ALLOY AT 1600 AND 2000 F

Closure of the capsules was accomplished by welding end plugs in place in a helium-filled dry box. The capsules, each of which contained two specimens, were placed in a stainless steel can which had a thermocouple well so fixed that temperature measurements could be made at the center of the capsule-containing shell. Tests were run in duplicate.

Specimens tested in NaK were examined and weighed after exposures of 156, 656, and 1000 hr. A summary of data obtained is shown in Table 12. Representative specimens of niobium-uranium alloys before and after exposure are shown in Figure 23. Specimens tested in sodium at 1500 F were examined after exposures of 500, 1000, and 1500 hr. The weight-change data for these tests are shown in Table 13. Figure 24 shows representative specimens of the niobium-uranium alloys before and after exposure to sodium. The surfaces of specimens prior to testing were quite rough. The surfaces were tested in this condition so that the maximum surface area would be exposed. No gross surface attack by either NaK or sodium occurred as is shown by the macrographs; the stain observed was introduced during cleaning.

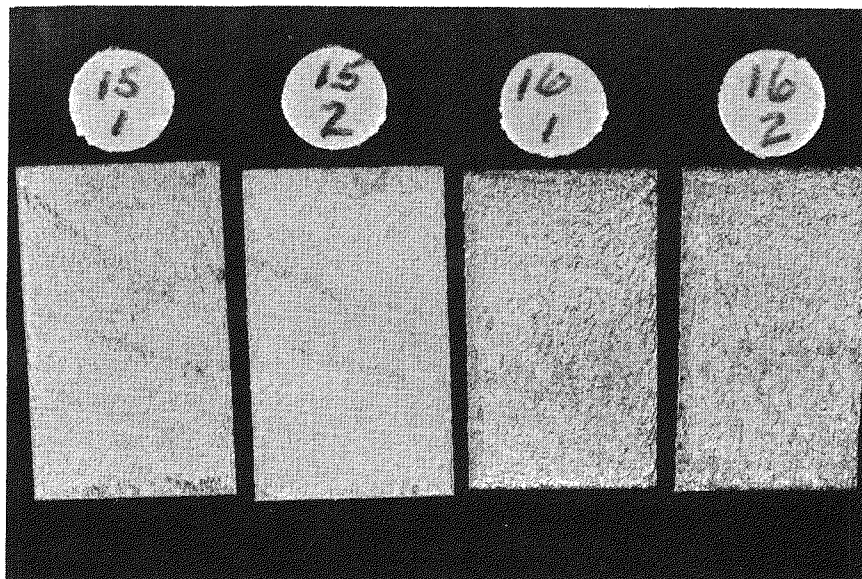
TABLE 12. CORROSION DATA FOR NIOBIUM-URANIUM ALLOYS<sup>(a)</sup> IN NaK AT 1600 F

Alloy Composition (Balance Niobium), w/o	Impurity Content		Specimen Condition	Total Weight Change, mg per cm <sup>2</sup> , After Indicated Time		
	Oxygen <sup>(b)</sup> , ppm	Zirconium <sup>(c)</sup> , w/o		156 Hr	656 Hr	1000 Hr
10 U	680	0.74	Fabricated	0	0.17	0.14
	1190	0.17	Fabricated	-0.66	0.05	-1.01
	3170	0.02	Fabricated	-0.33	-0.03	-0.31
20 U	458	0.74	Fabricated	0.92	0.37	1.25
	523	0.17	Fabricated	0.67	0.14	0.93
	198	0.02	Fabricated	0.31	0.25	0.69
30 U	165	0.02	As cast	0.93	0.52	2.09
40 U	261	0.02	As cast	1.48	0.38	2.51
50 U	271	0.02	As cast	0.96	0.55	2.50
60 U	192	0.02	As cast	1.36	1.15	3.24

(a) Values are averages from two specimens.

(b) Analyzed values.

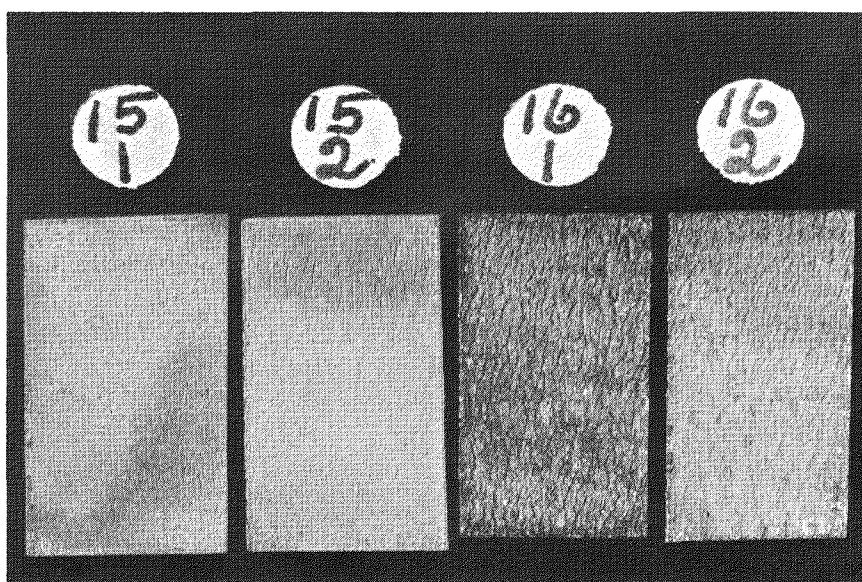
(c) Nominal composition.



2X

RM12978

a. Before Exposure to NaK



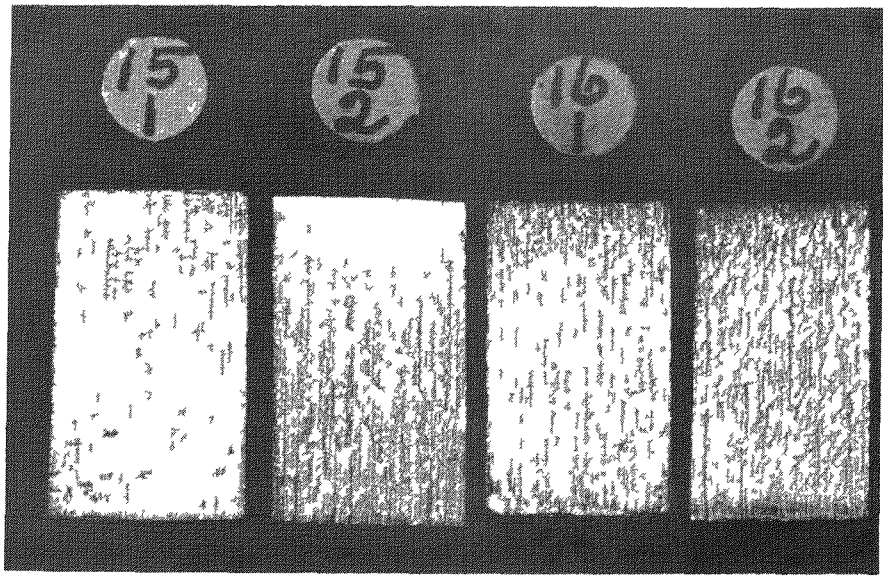
2X

RM14752

b. After Exposure to NaK at 1600 F for 1000 Hr

FIGURE 23. NIOBIUM-10 AND -20 w/o URANIUM ALLOYS BEFORE AND  
AFTER EXPOSURE TO NaK AT 1600 F

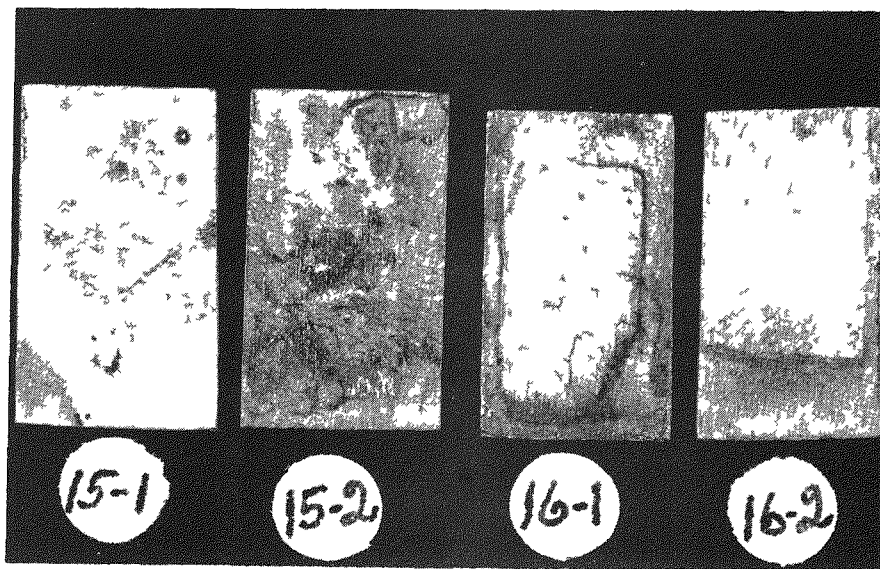
Specimens 16-1 and 16-2 were niobium-10 w/o uranium alloys;  
Specimens 15-1 and 15-2 were niobium-20 w/o uranium alloys.



2X

a. Before Exposure to Sodium

RM14829



2X

b. After Exposure to Sodium at 1500 F for 1500 Hr

RM16582

FIGURE 24. NIOBIUM-10 AND -20 w/o URANIUM ALLOYS BEFORE  
AND AFTER EXPOSURE TO SODIUM AT 1500 F

Specimens 16-1 and 16-2 are niobium-10 w/o uranium alloys,  
Specimens 15-1 and 15-2 are niobium-20 w/o uranium alloys.

TABLE 13. CORROSION DATA FOR NIOBIUM-URANIUM ALLOYS<sup>(a)</sup>  
EXPOSED TO SODIUM AT 1500 F

Alloy Content (Balance Niobium), w/o	Impurity Content		Specimen Condition	Total Weight Change, mg per cm <sup>2</sup> , After Indicated Time		
	Oxygen <sup>(b)</sup> , ppm	Zirconium <sup>(c)</sup> , w/o		500 Hr	1000 Hr	1500 Hr
10 U	680	0.74	Fabricated	0.03	-0.06	-0.08
	1190	0.17	Fabricated	0.05	0.07	0.15
	3170	0.02	Fabricated	-0.10	-0.41	-0.41
20 U	458	0.74	Fabricated	0.15	-0.30	-1.04
	523	0.17	Fabricated	0.17	0.52	0.64
	198	0.02	Fabricated	-0.04	0.10	0.10
30 U	165	0.02	As cast	0.18	0.89	1.70
40 U	261	0.02	As cast	0.55	1.78	2.32
50 U	271	0.02	As cast	0.49	3.32	4.45

(a) Values are averages from two specimens.

(b) Analyzed values.

(c) Nominal composition.

The source of the weight changes which occur during exposure is the oxygen contained in the sodium and NaK. Both contained approximately 50 ppm oxygen with the oxygen being reintroduced during each capsule opening for weight measurements. Examination of the weight-change data for the NaK and sodium exposures indicates that increased weight gains accompany increases in uranium content. This is illustrated graphically in Figure 25, which shows a plot of weight gain versus uranium content.

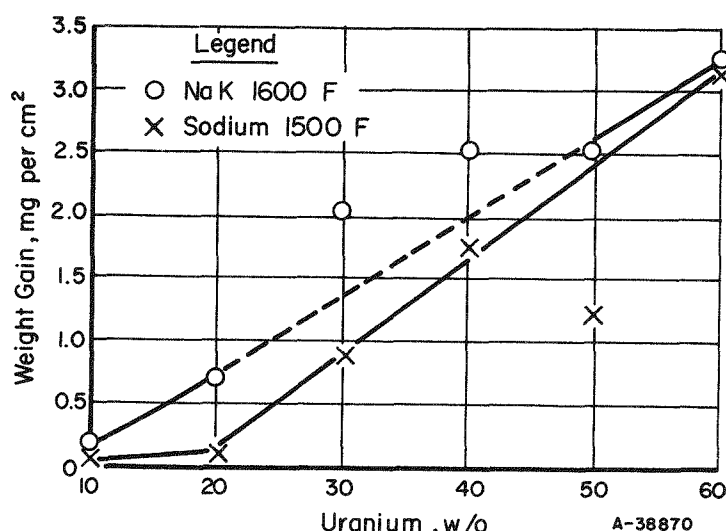


FIGURE 25. EFFECT OF INCREASING URANIUM CONTENT ON WEIGHT GAIN OF NIOBIUM IN NaK AT 1600 F AND SODIUM AT 1500 F FOR 1000-HR TEST

Specimens tested in sodium were examined metallographically to determine the extent, if any, of oxygen penetration. Figures 26a and 26b show a cross-sectional view of the niobium-10 and -20 w/o uranium alloys respectively. No obvious penetration or oxide layer was noted in these alloys. Apparently, the weight gains observed are a result of either or both the formation of a very thin surface oxide or the solution of oxygen in the alloys. While oxygen is fairly soluble in niobium, it is expected that the addition of uranium will decrease this solubility, although the extent of the decrease cannot be predicted.

Figure 27 shows the surface of the niobium-60 w/o uranium sample which had experienced a large weight gain. This particular alloy sample was tested in the as-cast condition and dark appearing uranium-rich dendrites are seen in the bulk of the material. However, a change in structure is observed in the area just below the surface of the specimen. In the higher magnification in the as-polished condition, it is evident that this change in structure is the result of internal oxidation. It appears that the uranium-rich dendrites provide a path for oxygen diffusion which leads to the probable formation of uranium dioxide.

These results indicate that niobium-uranium alloys containing less than 60 w/o uranium are highly resistant to attack by either NaK or sodium even if oxygen is present in the liquid metal. In the absence of oxygen, little attack by either sodium or NaK would be expected.

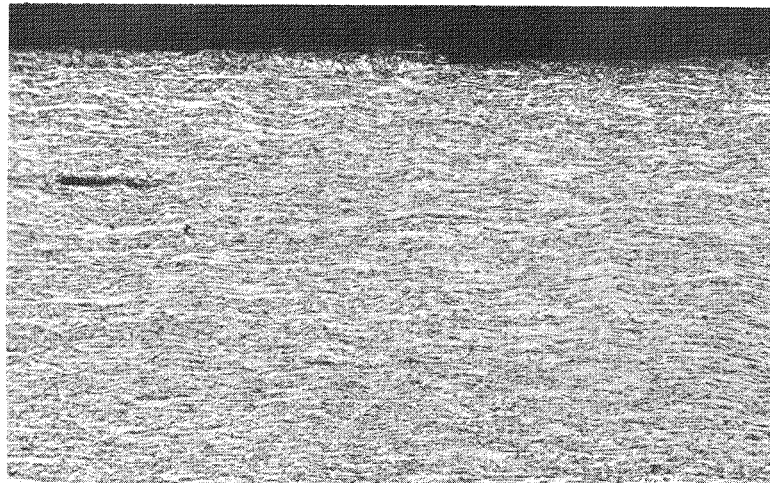
The above experimental results indicate that the niobium-uranium alloys containing less than 60 w/o uranium are highly resistant to attack by either NaK or sodium and, in fact, would probably remain relatively unaffected if exposed to oxygen-free NaK or sodium.

#### In Water

Tests in 600 and 680 F water were conducted for 336 and 140 days, respectively. Plate-type specimens were prepared for testing by machining approximately 0.0007 in. from each specimen surface and pickling in a solution of nitric acid, water, and HF to remove an additional 0.0002 in. from the surface. The specimens were then weighed and placed in autoclaves for testing. All tests were performed in duplicate.

In order to evaluate the effect of impurity content on corrosion behavior of the alloys, vacuum-fusion and chemical analyses were obtained on material which was taken from the area adjacent to that from which the test specimens were prepared. These analyses are shown in Table 14. A majority of the niobium-uranium specimens contain less than 600 ppm oxygen, although a few contain over 1000 ppm.

A summary of weight changes observed in 600 F water for 336 days of exposure is shown in Table 15. Although specimens were examined and weighed every 14 days, only data for 1-month intervals are shown. No obvious trend in corrosion rate with change in uranium content up to 50 w/o uranium is apparent from the data. However, the 60 w/o uranium alloy shows a definitely higher corrosion weight loss as compared with the remaining alloys. Also, from the data for the 10 w/o uranium alloy, it can be concluded that corrosion resistance decreases when oxygen content becomes excessive, greater than about 1000 ppm for this particular alloy.



100X

RM16676

## a. Niobium-10 w/o Uranium Alloy

No penetration occurred. Structure is that of heavily worked material. Alloy contained 680 ppm oxygen. Total weight gain was 0.15 mg per  $\text{cm}^2$ .



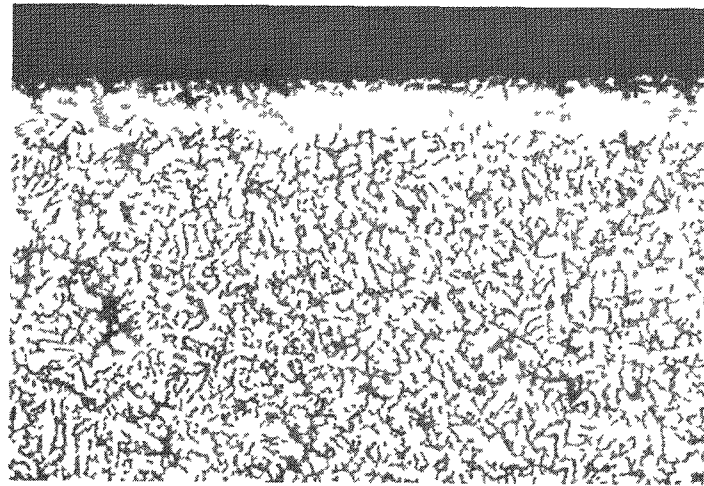
100X

RM16932

## b. Niobium-20 w/o Uranium Alloy

No penetration occurred. Structure is that of heavily worked material. Alloy contained 198 ppm oxygen. Total weight gain was 0.10 mg per  $\text{cm}^2$ .

FIGURE 26. NIOBIUM-10 AND -20 w/o URANIUM ALLOYS EXPOSED TO SODIUM AT 1500 F FOR 1500 HR

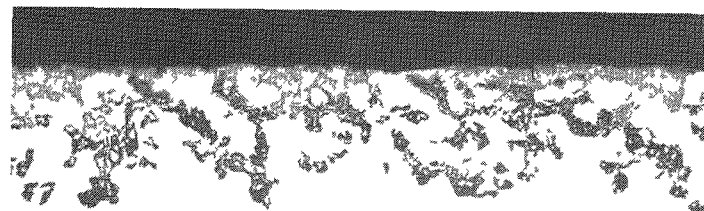


100X

Etched

RM16668

a. Extensive Dendritic Structure and Oxygen-Affected Zone at the Surface



250X

As Polished

RM17451

b. Evidence of Internal Oxidation

FIGURE 27. NIOBIUM-60 w/o URANIUM ALLOY EXPOSED TO SODIUM AT 1500 F FOR 1500 HR

Material was in the as-cast condition. Alloys contained 192 ppm oxygen prior to testing.

TABLE 14. PRECORROSION CHEMICAL ANALYSIS OF NIOBIUM-URANIUM SPECIMENS

Alloy Composition, (Balance Niobium), w/o	Impurity Content of Niobium Melting Stock, ppm				Condition	Analyzed Impurity Content of Alloy Before Exposure, ppm			
	Oxygen	Hydrogen	Nitrogen	Carbon		Oxygen	Hydrogen	Nitrogen	Carbon
10 U	600	--	580	280	Fabricated	680	9	900	340
	700	--	600	270	Fabricated	1190	3	780	340
	300	--	300	100	Fabricated	3170	7	780	80
20 U	600	--	580	280	Fabricated	458	7	1600	370
	700	--	600	270	Fabricated	523	10	1000	330
	300	--	300	100	Fabricated	198	19	340	60
30 U	600	--	580	280	As cast	586	62	850	420
	700	--	600	270	Fabricated	669	12	410	250
	300	--	300	100	As cast	165	39	120	50
40 U	600	--	580	280	As cast	661	7	320	310
	700	--	600	270	As cast	579	2	330	230
	300	--	300	100	As cast	261	0.7	130	20
50 U	600	--	580	280	As cast	375	7	270	260
	700	--	600	270	As cast	334	4	260	280
	300	--	300	100	As cast	271	2	130	300
60 U	600	--	580	280	As cast	471	9	230	190
	700	--	600	270	As cast	273	3	200	190
	300	--	300	100	As cast	192	3	120	80

TABLE 15. CORROSION DATA FOR NIOBIUM-

Alloy Composition (Balance Niobium), w/o	Impurity Content		Specimen Condition				
	Oxygen <sup>(b)</sup> , ppm	Zirconium <sup>(c)</sup> , w/o		7	28	56	84
10 U	680	0.74	Fabricated	0.12	0.28	0.40	0.62
	1190	0.17	Fabricated	0.25	0.48	0.74	1.05
	3170	0.02	Fabricated	0.29	0.53	0.82	1.10
20 U	458	0.74	Fabricated	0.18	0.42	0.64	1.06
	523	0.17	Fabricated	0.25	0.49	0.78	1.08
	198	0.02	Fabricated	0.18	0.33	0.51	0.76
30 U	586	0.74	As cast	0.31	0.53	0.78	0.94
	669	0.17	Fabricated	0.27	0.42	0.76	0.76
	165	0.02	As cast	0.31	0.64	1.03	1.43
40 U	661	0.74	As cast	0.52	0.83	1.03	0.78
	579	0.17	As cast	0.29	0.50	0.63	1.01
	261	0.02	As cast	0.23	0.40	0.61	1.04
50 U	375	0.74	As cast	0.24	0.47	0.68	0.96
	334	0.17	As cast	0.25	0.46	0.62	0.80
	271	0.02	As cast	0.26	0.46	0.55	0.95
60 U	471	0.74	As cast	0.27	0.42	0.18	-0.48
	273	0.17	As cast	0.31	0.48	0.62	0.50
	192	0.02	As cast	0.20	0.36	0.46	0.58
100 Nb	131	0.05	Fabricated	--	--	--	0.53
Zircaloy-2	--	--	Fabricated	0.09	0.12	0.14	0.16

(a) Average of duplicate specimens.

(b) Analyzed value.

(c) Nominal composition.

URANIUM ALLOYS<sup>(a)</sup> IN WATER AT 600 F

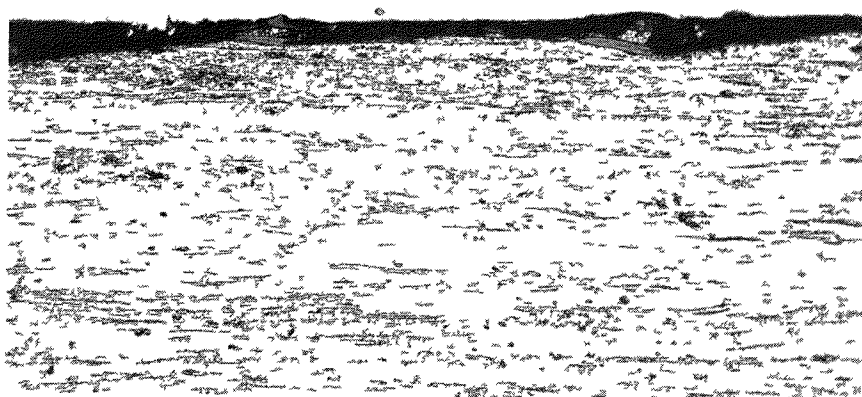
Total Weight Change, mg per cm <sup>2</sup> , After Indicated Number of Days								
112	140	168	196	224	252	280	308	336
0.70	0.61	0.60	0.61	0.63	0.73	0.61	0.71	0.81
0.90	0.60	-0.59	-1.12	-0.76	-1.23	-3.45	-3.92	-4.56
0.62	0.38	-1.52	-2.20	-3.51	-3.93	-5.03	-5.46	-6.03
1.20	1.14	0.98	0.96	0.95	0.93	0.92	1.05	1.14
1.34	1.35	1.64	1.90	1.93	2.33	1.99	1.32	0.82
0.84	0.71	0.69	0.73	0.76	0.76	0.73	0.80	0.86
0.87	0.74	0.53	0.15	0.10	-0.11	-0.41	-0.40	-0.63
0.54	-0.25	-1.28	-2.15	-2.32	-2.75	-2.78	-2.79	-2.78
1.02	1.07	0.40	-0.78	-0.59	-0.86	-1.61	-1.30	-1.25
0.75	0.49	0.49	0.43	0.43	0.63	0.63	0.40	0.20
0.75	0.47	0.28	0.20	0.20	0.23	0.03	0.07	0.18
0.89	0.77	0.57	0.61	0.62	0.75	0.53	0.67	0.96
1.00	0.87	0.61	0.31	0.15	-0.17	-0.53	-0.77	-1.16
0.92	0.66	0.53	0.40	0.37	0.24	-0.06	-0.07	-0.11
0.59	0.38	0.04	-0.31	-0.54	-0.88	-1.45	-1.82	-2.62
-1.21	-2.12	-3.28	-4.70	-6.02	-7.53	-8.76	-10.63	-12.60
0.03	-1.32	-2.80	-4.23	-5.44	-6.47	-7.34	-8.16	-9.50
-0.38	-0.18	-0.76	-1.27	-1.67	-2.16	-2.78	-3.67	--
0.63	0.67	0.75	0.79	0.73	0.89	0.76	0.70	--
0.20	0.22	--	--	0.24	0.26	0.28	0.32	--



250X

RM17452

a. As Polished



250X

RM16929

b. Etched

FIGURE 28. NIOBIUM-10 w/o URANIUM ALLOY EXPOSED TO  
600 F WATER FOR 336 DAYS

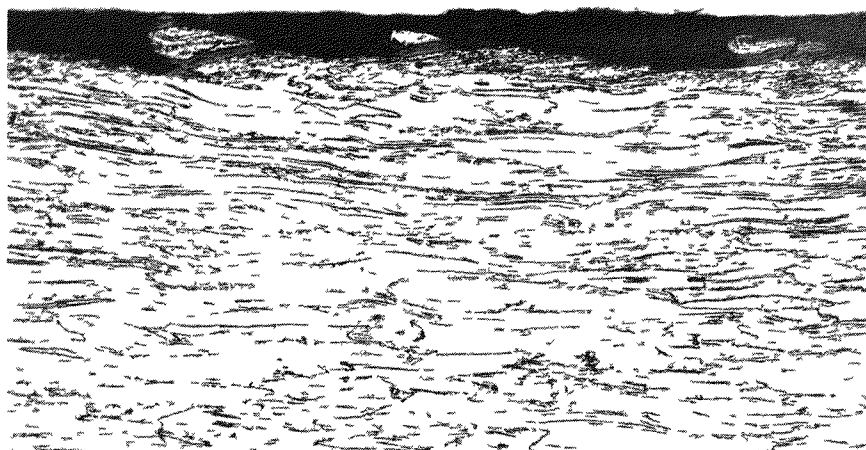
No oxide penetration into the structure is apparent.  
Specimen showed a total weight gain of 0.81 mg per  
cm<sup>2</sup>. Slight surface oxide is visible.



250X

RM17450

a. As Polished



250X

RM16928

b. Etched

FIGURE 29. NIOBIUM-20 w/o URANIUM ALLOY EXPOSED TO 600 F  
WATER FOR 336 DAYS

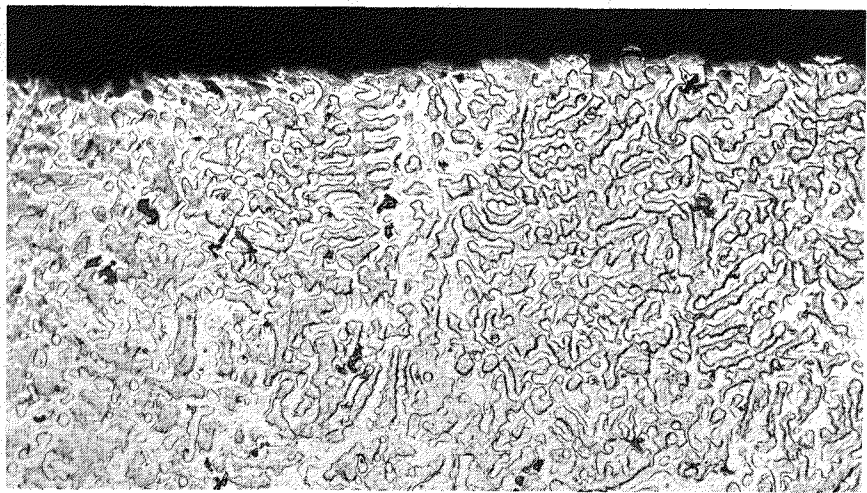
No oxide penetration into structure is apparent.  
Specimen showed a total weight gain of 86 mg per  
cm<sup>2</sup>. Slight surface oxide is visible.



250X

RM17449

a. As Polished



250X

RM16931

b. Etched

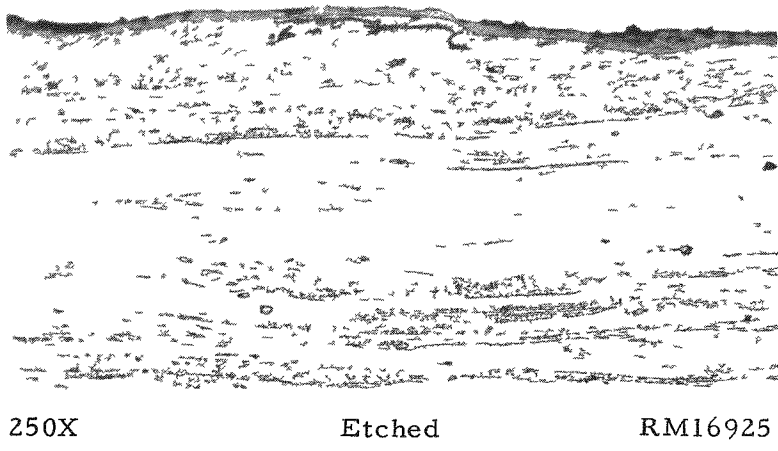
FIGURE 30. NIOBIUM-50 w/o URANIUM ALLOY EXPOSED TO  
600 F WATER FOR 336 DAYS

No oxide penetration into structure is apparent.  
Specimen showed a total weight loss of 0.11 mg  
per  $\text{cm}^2$ . Structure is as cast and shows dendrites.

The surfaces of niobium-10, -20, and -50 w/o uranium specimens are shown in Figures 28, 29, and 30, respectively, in both the as-polished and etched condition. These micrographs show a slight oxide film but no apparent penetration. The niobium-10 and -20 w/o uranium alloys were tested in a cold-worked condition while the niobium-50 w/o uranium alloy was in the as-cast condition. The structure of the 50 w/o uranium alloy, Figure 30, shows dendrites formed during solidification.

As would be expected, more extensive attack by water (Table 16) was observed at 680 F. After 140 days' exposure, almost all of the alloys showed weight losses. In order to determine if there was any correlation between hydrogen pickup and corrosion, samples of each alloy were analyzed for hydrogen. Table 17 lists the changes in hydrogen content and total weight gain of hydrogen. Evaluation of data shown in this table indicates that in the high-niobium alloys (niobium-10, -20, and -30 w/o uranium), excessive weight losses are accompanied by large increases in hydrogen content; however, in the remaining alloys (niobium-40, -50, and -60 w/o uranium) the weight loss does not appear to be related to hydrogen pickup. The corrosion mechanism for the niobium-uranium alloys probably changes with increasing uranium content with the role of hydrogen in corrosion becoming negligible in the higher uranium alloys.

The microstructure of the niobium-10 w/o uranium alloy which lost 1.66 mg per  $\text{cm}^2$  after 140 days' exposure is shown in Figure 31. An oxide layer can be observed on the surface.



RM16925

FIGURE 31. NIOBIUM-10 w/o URANIUM ALLOY EXPOSED TO 680 F WATER FOR 140 DAYS

Continuous surface oxide is visible. Specimen showed a weight loss of 1.66 mg per  $\text{cm}^2$ .

The niobium-20 w/o uranium alloy appears to possess the best corrosion resistance in both 600 and 680 F water of the niobium-uranium alloys tested. Figure 32 shows a plot of the corrosion behavior of this alloy in 600 and 680 F water as compared with that of Zircaloy-2 in 680 F water. In 600 F water the alloy shows a slight weight increase which levels off quickly; very little change in weight is noted up to 336 days after the initial increase. In 680 F water, the niobium-20 w/o uranium alloy shows a steady

TABLE 16. CORROSION DATA FOR NIOBIUM-

Alloy Composition (Balance Niobium), w/o	Impurity Content		Specimen Condition		
	Oxygen <sup>(b)</sup> , ppm	Zirconium <sup>(c)</sup> , w/o		7	14
10 U	680	0.74	Fabricated	0.28	0.32
	1190	0.17	Fabricated	0.09	-1.52
	3170	0.02	Fabricated	-4.22	-14.3
20 U	458	0.74	Fabricated	0.30	0.48
	523	0.17	Fabricated	0.43	0.68
	198	0.02	Fabricated	0.22	0.38
30 U	586	0.74	As cast	1.00	1.19
	669	0.17	Fabricated	0.97	0.88
	165	0.02	As cast	0.50	0.70
40 U	661	0.74	As cast	0.66	0.75
	579	0.17	As cast	0.46	0.43
	261	0.02	As cast	0.46	0.65
50 U	375	0.74	As cast	0.83	0.47
	334	0.17	As cast	0.44	0.39
	271	0.02	As cast	0.38	0.27
60 U	471	0.74	As cast	1.86	-24.0
	273	0.17	As cast	0.57	-0.26
	192	0.02	As cast	0.31	-0.02
100 Nb	131	0.05	Fabricated	--	0.79
	500	0.03	Fabricated	--	0.41
Zircaloy-2	--	--	Fabricated	--	0.15

(a) Average of duplicate specimens.

(b) Analyzed values.

(c) Nominal compositions.

(d) Both specimens taken off tests.

(e) Completely oxidized after 56 days of exposure.

URANIUM ALLOYS<sup>(a)</sup> IN 680 F WATER

Total Weight Change, mg per cm <sup>2</sup> , After Indicated Number of Days								
28	42	56	70	84	98	112	124	140
0.28	0.23	0.16	0.65	0.72	0.11	-0.20	-0.49	-1.66
-3.66	-5.66	-7.67	-9.2	-10.1	-11.2	-13.6	-15.0	-17.7
-23.8	-31.8	-38.5	-35.7	-37.7	-39.9	-42.5	-45.0	-48.2
0.61	0.74	0.91	1.06	1.18	0.67	0.60	0.08	-0.58
1.05	1.20	1.58	1.67	1.44	0.54	-1.38	-5.47	-10.0
0.55	0.66	0.89	1.03	1.09	0.87	0.93	0.60	0.05
0.38	0.21	-0.84	-0.71	-0.76	-0.90	-0.77	-0.89	-1.16
0.43	-0.43	-0.75	-0.91	-0.89	-1.08	-1.03	-1.78	-1.66
0.68	-0.82	-1.67	-2.34	-2.46	-2.55	-2.48	-2.50	-2.74
1.00	1.08	1.41	1.53	1.72	1.54	1.60	-0.03	1.01
0.30	0.29	0.51	0.77	0.78	0.51	1.29	1.01	0.67
0.80	1.05	1.30	1.47	1.70	1.78	1.61	-2.52	-2.66
0.29	0.29	0.39	1.44	0.0	-0.72	-0.97	-1.58	-2.66
0.40	0.23	0.09	0.42	0.42	-0.48	-1.43	-1.95	-2.81
None	0.12	-1.92	-2.90	-3.96	-4.84	-6.57	-7.20	-8.18
-31.5	-39.0	-57.6	-69.5	(d)	--	--	--	--
-2.4	-4.29	5.95	-8.1	-9.55	-11.3	-13.0	-14.5	-17.4
-1.15	-2.41	3.50	-5.1	-6.20	-7.76	-9.07	-10.17	-12.4
1.00	-1.07	--	--	--	--	--	--	--
-1.36	-46.8	(e)	--	--	--	--	--	--
0.20	0.23	0.23	0.24	0.30	0.34	0.38	0.42	0.48

TABLE 17. RESULTS OF ANALYSES<sup>(a)</sup> FOR HYDROGEN CONTENT OF NIOBIUM-URANIUM ALLOYS AFTER 140 DAYS IN 680 F WATER

Alloy Composition (Balance Niobium), w/o	Analyzed Oxygen Content, ppm	Hydrogen Content, ppm		Total Weight Gain of Hydrogen, mg per cm <sup>2</sup>	Total Weight Change, mg per cm <sup>2</sup>
		Before Exposure	After Exposure <sup>(b)</sup>		
10 U	680	9	155	0.011	-1.66
	1190	3	870	0.27	-17.7
	3170	7	1510	0.51	-48.2
20 U	458	7	89	0.028	-0.58
	523	10	790	0.415	-10.0
	198	19	47	0.026	0.05
30 U	586	62	127	0.011	-1.16
	669	12	66	0.054	-1.66
	165	39	21	-0.028	-2.74
40 U	661	7	52	0.038	1.01
	579	2	46	0.038	0.67
	261	0.7	10	0.009	-2.66
50 U	375	7	28	0.02	-2.66
	334	4	16	0.017	-2.81
	271	2	23	0.017	-8.18
60 U	471	9	(c)	--	(c)
	273	3	66	0.05	-17.4
	192	3	35	0.02	-12.4

(a) Vacuum-fusion method.

(b) Performed on unabraded surfaces.

(c) Specimens lost in tests after 70 days.

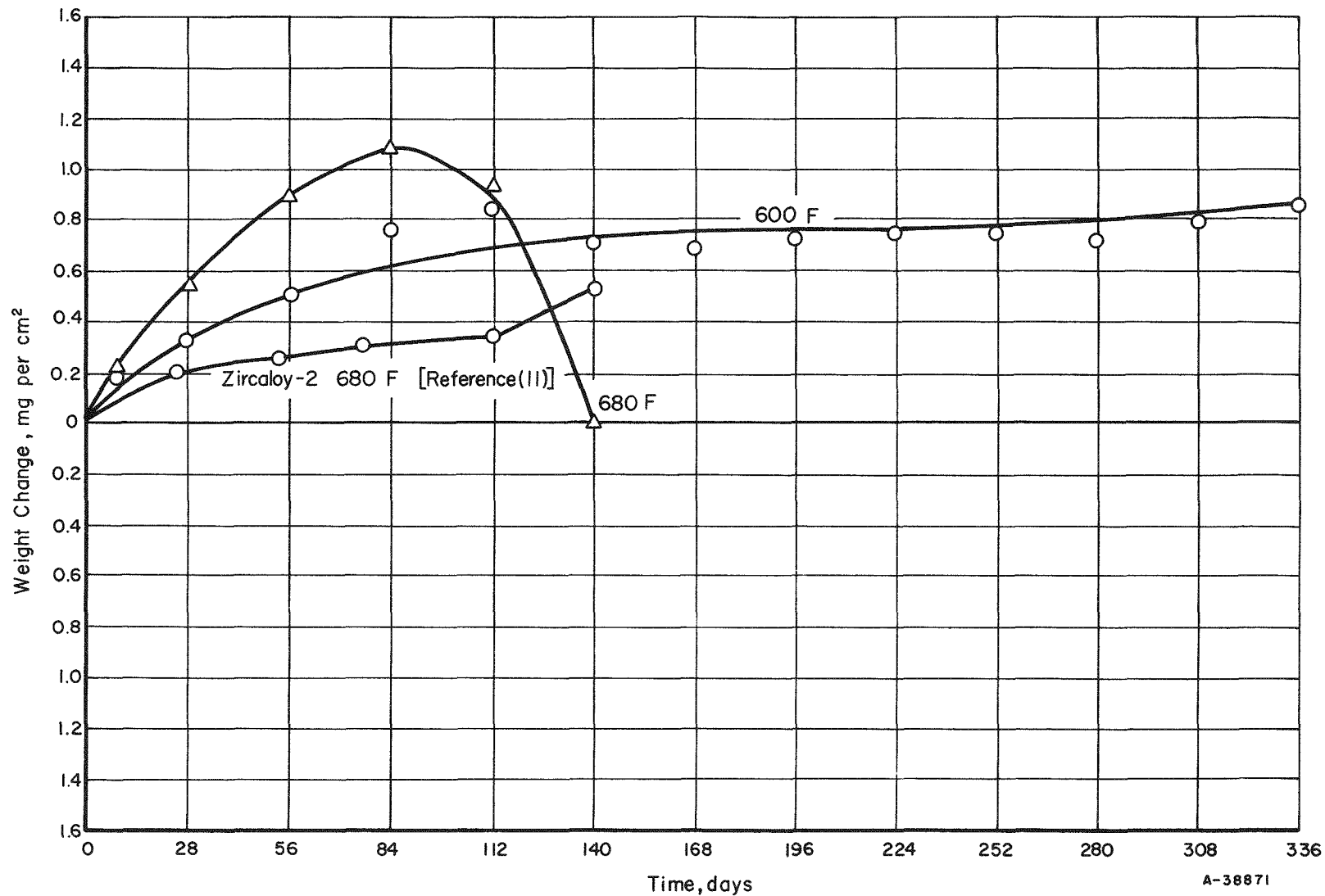


FIGURE 32. EFFECT OF TIME ON WEIGHT CHANGES OF NIOBIUM-20 w/o URANIUM ALLOY IN 600 AND 680 F WATER

increase in weight up to 84 days, at which time the alloy begins to lose weight. At this point, the oxide layer has ceased to be adherent and begins to spall. It continued to spall for the remaining time to 140 days' exposure at which point the specimen was removed from test.

All of the niobium-uranium alloys tested appear to possess adequate corrosion resistance to 600 and 680 F water so that defects in cladding which might occur would not be serious for relatively long periods of time.

#### PHYSICAL-PROPERTY DETERMINATIONS

##### Thermal-Conductivity Measurements

Thermal-conductivity measurements were made by a steady-heat-flow method which consists of heating one end of a specimen, measuring the temperature gradient along the specimen, and determining the rate of heat flow through the specimen by means of a metal standard (Armco iron) of known thermal conductivity attached to the cold end of the specimen. Radial heat flow into or away from the specimen is kept to a minimum by thermal insulation and an encircling guard tube. Tests were performed under a vacuum of approximately  $2 \times 10^{-5}$  mm of mercury. Five Chromel-Alumel thermocouples in the niobium-20 w/o uranium alloy specimen and four in the niobium-10 w/o uranium alloy specimen were wedged in equally spaced holes along the specimen. Two thermocouples were also placed in the Armco iron standard.

Figure 33 shows the thermal conductivity of unalloyed niobium and the niobium-10 and -20 w/o uranium alloys from room temperature to 1800 F. Alloying uranium with niobium results in decreased thermal conductivity. This effect is more pronounced at room temperature than at elevated temperatures.

##### Electrical-Resistivity Measurements

Electrical-resistivity measurements were made on the niobium-10 and -20 w/o uranium alloys by the potentiometric method using a specimen approximately 1 in. long. Steel points pressed against the specimen were used as potential leads; copper wires clamped to the ends of the specimens served as current leads. Measurements were made under a vacuum of about  $5 \times 10^{-5}$  mm of mercury. Results of resistivity measurements are shown in Figure 34. As can be seen, the addition of uranium to niobium significantly increases the resistivity of unalloyed niobium.

Since the thermal conductivity and electrical conductivity (reciprocal of electrical resistivity) of a metal depend upon the presence of free electrons, there should be a relatively simple relationship between the two. Wiedemann and Franz<sup>(12)</sup> proposed that the ratio  $K/\sigma$ , where  $K$  is the thermal conductivity and  $\sigma$  is the electrical conductivity, should be constant. Lorenz later showed the above relationship to be temperature dependent and introduced  $T$ , the absolute temperature, to yield the constant  $K/\sigma T$ . Later

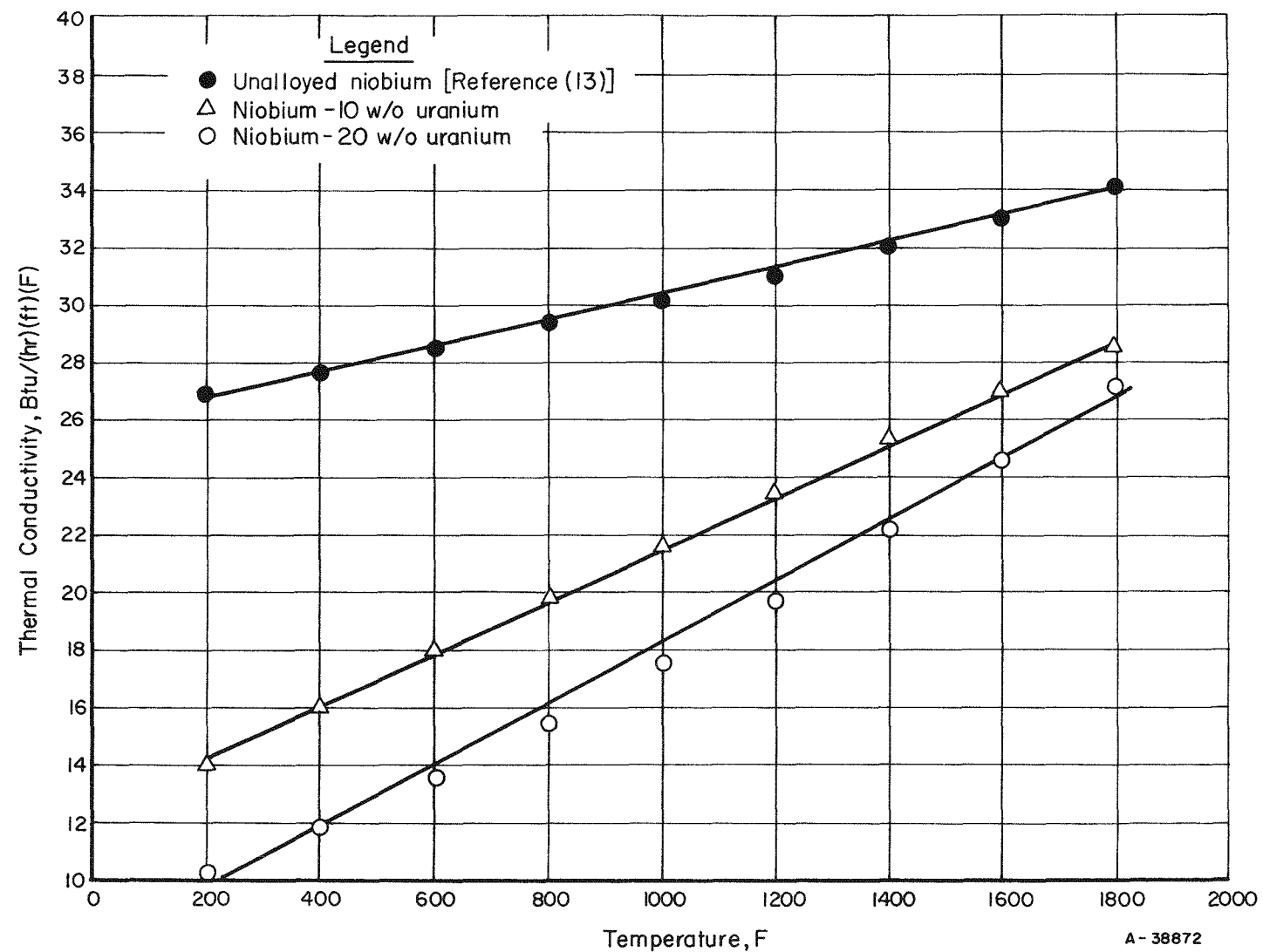


FIGURE 33. THERMAL CONDUCTIVITY OF NIOBIUM AND NIOBIUM-10 AND -20 w/o URANIUM ALLOYS

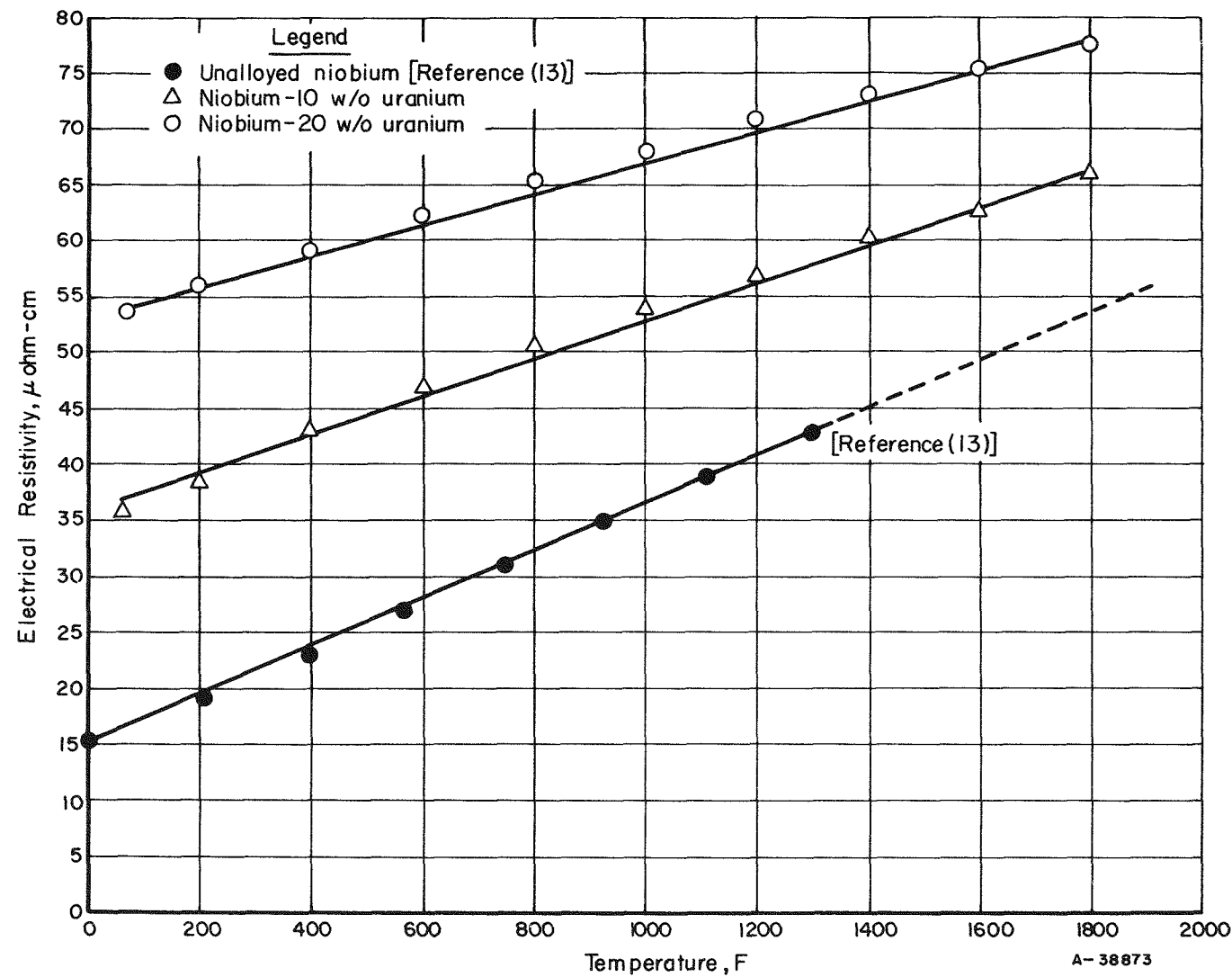


FIGURE 34. ELECTRICAL RESISTIVITY OF NIOBIUM AND NIOBIUM-10 AND -20 w/o URANIUM ALLOYS

work has shown that closer correlation between electrical and thermal conductivity can be obtained by adopting an equation of the form

$$K = A\sigma T + B,$$

where the constants A and B are determined empirically. In the above equation, the term  $A\sigma T$  is considered the contribution of electronic conduction and B is the contribution of lattice conduction to the total thermal conductivity. The usefulness of this equation lies in the ability to predict the thermal conductivity of a given alloy if the electrical conductivity of the alloy is known. In Figure 35 a plot is shown of the Wiedemann-Franz relation for niobium-uranium alloys. This curve was obtained by plotting the thermal conductivity versus the  $\sigma T$  where T is the temperature in degrees Kelvin. A least-square analysis of the data shown in Figures 33 and 34 yielded the equation  $K = 0.0124 + (0.0271) \sigma T$  as the best fit for the niobium-uranium system. As can be seen in Figure 35, the experimental curve also shows a reasonably good fit with the so-called "ideal" Wiedemann-Franz relation ( $K = 0.0245 \sigma T$ ).

#### Thermal-Expansion Measurements

Linear-thermal-expansion measurements shown in Figure 36 were made in a vertical quartz-tube recording dilatometer. Each specimen was thermal cycled twice from room temperature to about 1800 C and back to room temperature. Tests were performed in a vacuum of at least  $5 \times 10^{-5}$  mm of mercury. Alloying with 10 and 20 w/o uranium does not appear to significantly affect the thermal expansion of niobium.

#### Recrystallization Studies

The recrystallization behavior of the niobium-4.38, -10, -14.3, -20, -25, and -30 w/o uranium alloys was investigated. All alloys with the exception of the 30 w/o uranium alloy were reduced 90 per cent by rolling; the 30 w/o uranium alloy could only be reduced 80 per cent. Hardness measurements were obtained to serve as a rough indication of recrystallization with the extent of recrystallization being finally determined by metallographic examination.

Specimens of each alloy were annealed for 1 hr between 1800 and 2600 at 100 F intervals. Hardness measurements showed a large drop from room temperature to 1800 F (the lowest annealing temperature) with no additional decrease in hardness apparent upon increasing annealing temperatures to 2600 F. Major stress relief apparently occurs below 1800 F. This has been observed before with niobium-base alloys. (5)

In Figure 37 the microstructure of cold-worked niobium-14.3 w/o uranium is shown. This microstructure is typical of all the cold-worked alloys. A typical recrystallized microstructure is shown in Figure 38 for the niobium-30 w/o uranium alloy which was completely recrystallized at 2200 F. Table 18 lists the alloys studied and the temperatures at which recrystallization was completed.

In Figure 39, the microstructure of the niobium-10 w/o uranium alloy is shown. This alloy failed to completely recrystallize even at 3000 F. Recrystallization for this

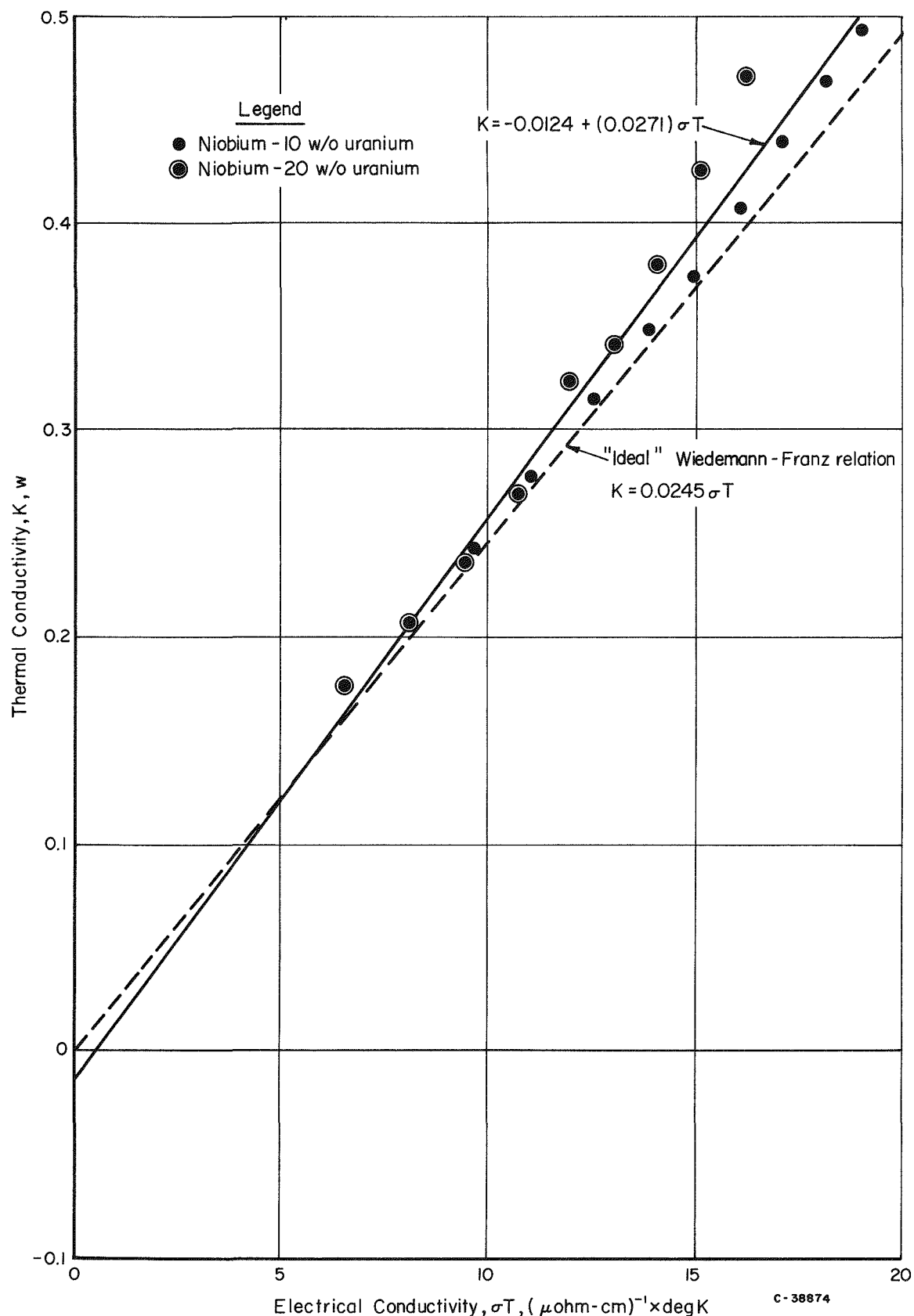


FIGURE 35. THERMAL AND ELECTRICAL CONDUCTIVITY RELATIONSHIPS FOR NIOBIUM-URANIUM ALLOYS

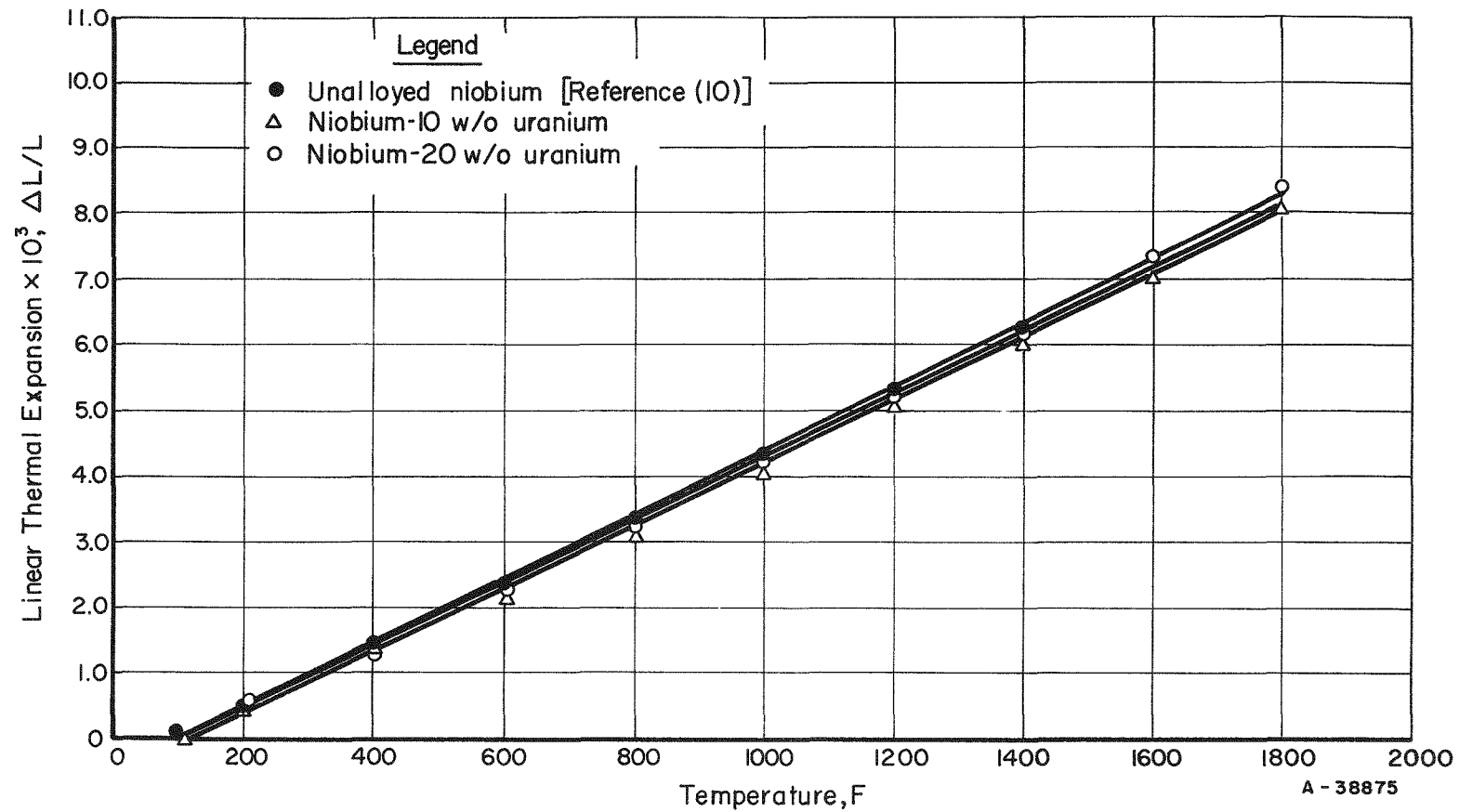
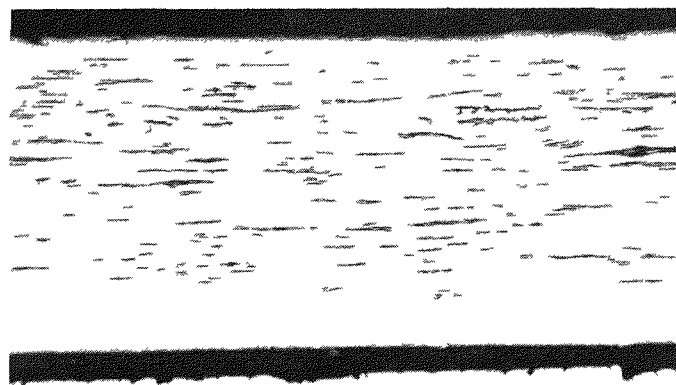


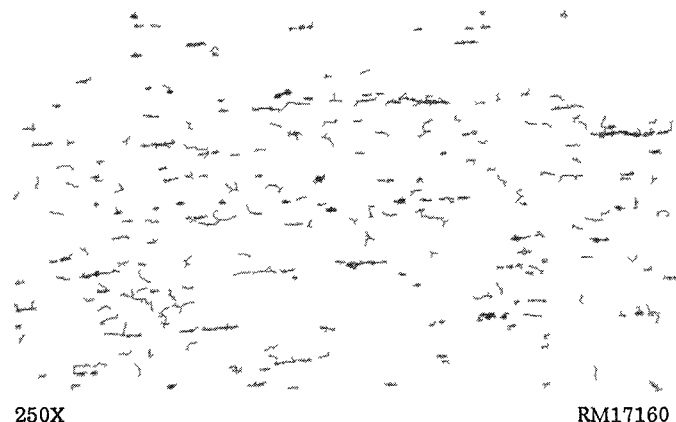
FIGURE 36. LINEAR THERMAL EXPANSION OF NIOBIUM AND NIOBIUM-10 AND -20 w/o URANIUM ALLOYS



250X RM19278

FIGURE 37. NIOBIUM-14.3 w/o URANIUM ALLOY COLD WORKED TO 90 PER CENT REDUCTION IN THICKNESS

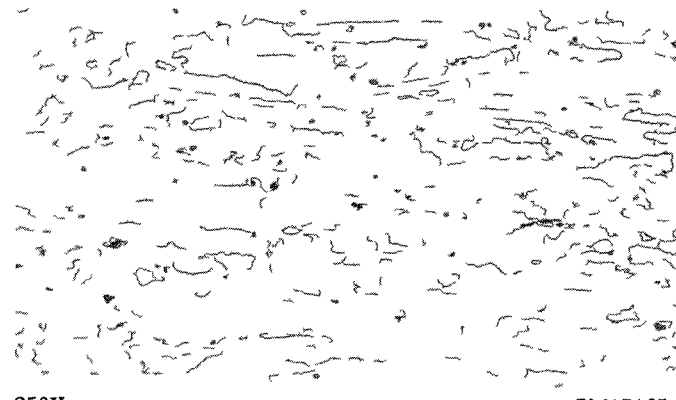
This structure is typical of the cold-worked niobium-uranium alloys.



250X RM17160

FIGURE 38. NIOBIUM-30 w/o URANIUM ALLOY COLD WORKED TO 80 PER CENT REDUCTION IN THICKNESS AND ANNEALED 1 HR AT 2200 F

Microstructure shows complete recrystallization.



250X RM17165

FIGURE 39. NIOBIUM-10 w/o URANIUM ALLOY COLD WORKED TO 90 PER CENT REDUCTION IN THICKNESS AND ANNEALED 1 HR AT 2400 F

High oxygen content (3100 ppm) of alloy is believed responsible for lack of recrystallization at temperatures to 3000 F.

TABLE 18. RECRYSTALLIZATION TEMPERATURES OF NIOBIUM-URANIUM ALLOYS

Alloy Composition (Balance Niobium), w/o	Cold Work, per cent	Temperature at Which Recrystallization is Complete
4.38 U	90	2300 F
10 U	92	Did not recrystallize at 3000 F (a)
14.3 U	90	2300 F
20 U	92	2400 F
25 U	90	2300 F
30 U	80	2200 F

(a) Alloy contained 3100 ppm oxygen.

alloy would be expected around 2300 F. Consequently, it appears that the high oxygen content of the alloy (3100 ppm) is preventing recrystallization with stress relief occurring before recrystallization can occur.

Uranium composition appears to have little effect on the recrystallization temperature in the range of compositions studied.

#### PHASE STUDIES

The effects of oxygen and zirconium on the composition limits of the gamma immiscibility loop in the niobium-uranium alloy system were also investigated. It is desirable to know the effects of oxygen and zirconium on niobium-uranium alloy structures since oxygen is a major impurity and zirconium a desirable alloying addition to niobium-uranium alloys. It was planned to compare the results obtained in this study with the composition limits of the gamma immiscibility loop determined from diffusion couples in a previous study. The two-phase region was established in this previous study on the basis of concentration-penetration curves determined by electron-microprobe analyses of the diffusion-annealed couples, as extending between 9 and 55 w/o niobium at 700 C, between 17 and 42 w/o niobium at 900 C, and between 21 and 37 w/o niobium at 925 C. At 1000 C, no two-phase immiscibility loop was detected in the diffusion couples.

In order to study the effects of oxygen on the gamma immiscibility loop, measured amounts of oxygen were added to sintered niobium initially containing about 200 ppm oxygen, by exposing the niobium to oxygen in a modified Sievert's apparatus. Three sets of alloy charges were then prepared: one set was prepared with the original niobium containing 200 ppm oxygen, a second set with niobium containing approximately 1000 ppm

oxygen, and a third set with niobium containing approximately 3000 ppm oxygen. The charges were prepared to produce alloys of uranium with nominally 10, 20, 30, 40, 50, 52, 54, 56, and 58 w/o niobium. To study the effects of zirconium, alloy charges of compositions niobium-60 w/o uranium-5, -10, and -20 w/o zirconium and niobium-50 w/o uranium-5, -10, and -20 w/o zirconium were prepared. The materials used in these alloys were sintered niobium biscuit, biscuit uranium, and crystal-bar zirconium.

The alloy charges were arc melted seven times for homogeneity and were cast into wire bars. In order to reduce any segregation that may have occurred during the casting of the alloys, the wire bars were annealed in vacuum for 8 hr at temperatures ranging from 1200 to 1600 C; the temperature of homogenization was varied depending on the niobium content of the alloy, being increased with increasing niobium content, except for the zirconium-bearing alloys which were all annealed at 1600 C.

Specimens for heat treatment were cut from the wire bars, wrapped in tantalum foil, and sealed in Vycor or quartz capsules, which were evacuated and which contained zirconium chips for gettering purposes. The heat treatments were chosen to bracket single-phase and two-phase regions in each group of alloy specimens heated together. The uranium-niobium alloys containing 10 w/o niobium were heated at temperatures ranging from 725 to 800 C for 1 month, the alloys containing 20, 30, and 40 w/o niobium were heated at temperatures ranging from 850 to 940 C for 1 month, the alloys containing 50 to 58 w/o niobium were heated at temperatures ranging from 650 to 750 C for 2 months, and the uranium-niobium-zirconium alloys were heated at temperatures ranging from 500 to 750 C for 3 months. All heat treatments were followed by water quenching.

After heat treatment, the alloys were metallographically examined. It was found that the alloys showed varying degrees of inhomogeneity and displayed dendritic structures; the most severe inhomogeneity was found to occur in the uranium-30 w/o niobium alloys. The uranium-10 w/o niobium alloys contained two phases, but second-phase platelets were distributed over only a small portion of the specimen surface. An attempt was made to utilize an electron-beam microanalyzer to establish the compositions of the  $\gamma_1$  matrix, and the  $\gamma_2$  platelets. However, the analyses were inconclusive since the  $\gamma_2$  platelets behaved nearly as two-dimensional surfaces which the electron-beam penetrated, resulting in misleading data. Because of the lack of homogeneity in the alloys, only conclusions which are qualitative in nature could be drawn from the observations.

In general, the structures of the heat-treated binary alloys were in agreement with the composition limits described by the diffusion analyses previously mentioned. Oxygen ranging from 100 to 1000 ppm by analysis for each alloy composition did not appear to appreciably affect the amounts of uranium- or niobium-rich second phase observed in the alloys. However, an additional oxide phase was evident in the alloys to which oxygen had been added. The uranium-20 w/o niobium and uranium-40 w/o niobium alloys contained, respectively, niobium-rich and uranium-rich second phase precipitated at the grain boundaries at temperatures up to 900 C; 940 C appeared to be the upper limit for second-phase precipitation in the uranium-30 w/o alloys. At 650 and 750 C, the uranium-52 w/o niobium alloys appeared to contain two phases, while the alloys containing 54 w/o niobium appeared to be single phase.

Alloys of niobium-50 w/o uranium with up to 10 w/o zirconium consisted primarily of retained gamma with massive transformation products at the grain boundaries. These

grain-boundary phases were produced by transformation of segregated uranium-rich areas to form alpha uranium and a niobium-rich solid solution. The alloys containing 60 w/o uranium did not contain grain-boundary transformation products but rather displayed random small areas where transformation had apparently occurred.

### CONCLUSIONS

In reviewing the information presented, the following conclusions can be drawn.

- (1) The inability to fabricate alloys containing 30 w/o or more uranium is probably due to segregation. Although skull melting eliminated banding or macrosegregation, it did not eliminate microsegregation.
- (2) Alloys of niobium containing 4.38 through 20 w/o uranium are much stronger in the 1600 to 2400 F range than a number of commonly used structural materials.
- (3) Contamination by oxygen results in increased tensile and creep strength up to 1600 F and reduced tensile elongation at temperatures up to 2200 F.
- (4) Creep tests of the niobium-uranium alloys indicate that high creep strength can be expected even at 2000 F.
- (5) Niobium-uranium alloys are compatible with NaK (1600 F) and sodium (1500 F). The slight attack which is noted in these liquids is due to the oxygen in the NaK and sodium.
- (6) The resistance of the niobium-uranium alloys to corrosion by 600 and 680 F water is adequate for a fuel material. Although there is some attack a cladding failure would not be expected to lead to catastrophic failure of the fuel.
- (7) Alloying with 10 and 20 w/o uranium decreases the thermal conductivity of unalloyed niobium in a manner typical of solid-solution alloys. A Wiedemann-Franz relation was developed which should allow reasonable predictions of the thermal conductivity of niobium-uranium alloys from electrical-resistivity data. The electrical resistivity of niobium is increased by the addition of 10 and 20 w/o uranium. Neither 10 nor 20 w/o uranium affect the thermal-expansion behavior of niobium significantly.
- (8) Recrystallization temperatures for alloys containing from 5 to 30 w/o uranium range from 2200 to 2400 F. High oxygen contamination appears to promote stress relief without recrystallization.

- (9) Oxygen additions produce no significant changes in niobium-uranium alloy constitution in the vicinity of the gamma immiscibility gap aside from the precipitation of oxide in the structure.

As a general conclusion, it can be stated that niobium-uranium alloys possess great promise for use as fuel alloys at elevated temperatures. They exhibit exceptional high-temperature strength and acceptable corrosion resistance to high-temperature water and liquid metals. However, fabricability problems limit consideration to alloys containing 25 w/o or less uranium.

Current irradiation studies remain to be completed to complete the evaluation of these alloys.

In addition to their promise as fuel alloys, the exceptional strength makes the high niobium (4 to 20 w/o uranium) alloys attractive as a structural material. The alloys mentioned above are readily fabricable, have excellent room-temperature ductility and in general possess a combination of properties rarely obtainable in materials exhibiting high elevated-temperature strength.

#### ACKNOWLEDGMENTS

The authors wish to thank Warren Berry for his helpful suggestions in interpretations of the water corrosion data. They would also like to acknowledge the help of Glenn Beatty in the determination of the Wiedemann-Franz relation for the niobium-uranium alloys.

#### REFERENCES

- (1) De Mastry, J. A., Shober, F. R., and Dickerson, R. F., "Metallurgical Studies of Niobium-Uranium Alloys", BMI-1400 (December 7, 1959).
- (2) Murr, W. E., and Melehan, J. B., private communication.
- (3) Rough, F. A., and Bauer, A. A., "Constitution of Uranium and Thorium Alloys", BMI-1300 (June 2, 1958).
- (4) Dickerson, R. F., Foster, E. L., and Chubb, W., "Segregation in Arc-Melted Uranium-Niobium Alloys", BMI-1218 (August 28, 1957). Confidential.
- (5) De Mastry, J. A., Shober, F. R., and Dickerson, R. F., "High-Temperature Niobium-Base Alloys for Sodium-Cooled Reactors", BMI-1513 (April 14, 1961).
- (6) Begley, R. T., and Platte, W. M., "Development of Niobium-Base Alloys", WADC TR 57-344, Part IV (February, 1960).
- (7) "Steels for Elevated Temperature Service", United States Steel (1949).

- (8) Hastelloy Alloy X, Haynes Stellite Company, Kokomo, Indiana (October, 1957).
- (9) "René 41", The Alloy Specialist, Cannon Muskegon Corporation.
- (10) Fieldhouse, I. B., Hedge, J. C., and Lang, J. I., "Measurement of Thermal Properties", WADC TR 58-274 (March 1, 1958).
- (11) The Metallurgy of Zirconium, National Nuclear Energy Series, McGraw-Hill Book Company, New York (1955), "Corrosion of Zirconium and Its Alloys" (B. Lustman).
- (12) Deem, H. W., Wood, W. D., and Lucks, C. F., "Memorandum on the Relationship Between Electrical and Thermal Conductivities of Titanium Alloys" (July 18, 1957).
- (13) Niobium Data Manual, E. L. Francis, Comp., IGR-R/R-304 (1958).

JAD:DPM:SGE:AAB:RFD/11s